



FEDERAL UNIVERSITY OF CEARÁ
DEPARTAMENT OF TELEINFORMATICS ENGINEERING
POSTGRADUATE PROGRAM IN TELEINFORMATICS ENGINEERING

MARCIEL BARROS PEREIRA

PARTICLE SWARM OPTIMIZATION AND DIFFERENTIAL
EVOLUTION FOR BASE STATION PLACEMENT WITH
MULTI-OBJECTIVE REQUIREMENTS

MASTER OF SCIENCE THESIS

ADVISOR: PROF. DR. FRANCISCO RODRIGO PORTO CAVALCANTI

CO-ADVISOR: PROF. DR. TARCISIO FERREIRA MACIEL

FORTALEZA – CEARÁ

JULY 2015

MARCIEL BARROS PEREIRA

PARTICLE SWARM OPTIMIZATION AND DIFFERENTIAL
EVOLUTION FOR BASE STATION PLACEMENT WITH
MULTI-OBJECTIVE REQUIREMENTS

Dissertação submetida à Coordenação do Programa de Pós-Graduação em Engenharia de Teleinformática, da Universidade Federal do Ceará, como requisito parcial para a obtenção do grau de **Mestre em Engenharia de Teleinformática**.

Área de Concentração: Sinais e Sistemas.

Orientador: Prof. Dr. Francisco Rodrigo Porto Cavalcanti

Co-orientador: Prof. Dr. Tarcisio Ferreira Maciel

UNIVERSIDADE FEDERAL DO CEARÁ
DEPARTAMENTO DE ENGENHARIA DE TELEINFORMÁTICA
PROGRAMA DE PÓS-GRADUAÇÃO EM ENGENHARIA DE
TELEINFORMÁTICA

FORTALEZA – CEARÁ

JULHO DE 2015

Dados Internacionais de Catalogação na Publicação
Universidade Federal do Ceará
Biblioteca de Pós-Graduação em Engenharia - BPGE

P493p

Pereira, Marciel Barros.

Particle swarm optimization and differential evolution for base station placement with multi-objective requirements / Marciel Barros Pereira. – 2015.

73 f. : il. color. , enc. ; 30 cm.

Dissertação (mestrado) – Universidade Federal do Ceará, Centro de Tecnologia, Departamento de Engenharia de Teleinformática, Programa de Pós-Graduação em Engenharia de Teleinformática, Fortaleza, 2015.

Área de concentração: Sinais e Sistemas.

Orientação: Prof. Dr. Francisco Rodrigo Porto Cavalcanti.

Coorientação: Prof. Dr. Tarcisio Ferreira Maciel.

1. Teleinformática. 2. Planejamento de redes celulares. 3. Otimização heurística. I. Título.

CDD 621.38

MARCIEL BARROS PEREIRA

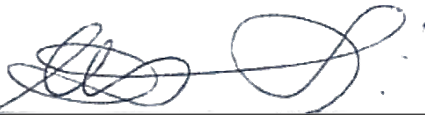
PARTICLE SWARM OPTIMIZATION AND DIFFERENTIAL EVOLUTION FOR
BASE STATION PLACEMENT WITH MULTI-OBJECTIVE REQUIREMENTS

Dissertação submetida à Coordenação do Programa de Pós-Graduação em Engenharia de Teleinformática, da Universidade Federal do Ceará, como requisito parcial para a obtenção do grau de **Mestre em Engenharia de Teleinformática**.

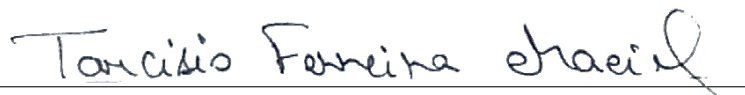
Área de Concentração: Sinais e Sistemas.

Aprovada em: 15/07/2015.

BANCA EXAMINADORA



Prof. Dr. Francisco Rodrigo Porto Cavalcanti
(*Orientador*)
Universidade Federal do Ceará



Prof. Dr. Tarcisio Ferreira Maciel
(*Coorientador*)
Universidade Federal do Ceará



Prof. Dr. Emanuel Bezerra Rodrigues
Universidade Federal do Ceará



Prof. Dr. Francisco Rafael Marques Lima
Universidade Federal do Ceará

In memoriam to my aunt Maria Salete and my grandparent Francisco Inácio, who raised me and taught me valuable lessons.

I'm a great believer that any tool that enhances communication has profound effects in terms of how people can learn from each other, and how they can achieve the kind of freedoms that they're interested in.

Bill Gates

ACKNOWLEDGEMENTS

To all people who have collaborated and helped me in the development of this thesis.

First, I would like to express my gratitude to my supervisor Professor Dr. Francisco Rodrigo Porto Cavalcanti for encouraging me to engage in the master's course and for supporting, teaching and guiding me during the supervision of my studies. I am grateful to my co-supervisor Professor Dr. Tarcisio Ferreira Maciel for the incentive, support, advices and encouragement to participate in a research project during my master.

To all my colleagues and friends enrolled to Wireless Communications Research Group – GTEL/UFC – which discussions, advices, suggestions and friendship were essential to the development of this work.

I am grateful to the GTEL group itself for welcoming me during my studies, for the infrastructure granted, and for the scholarship and travelling financial support. To the Postgraduate Program in Teleinformatics Engineering – PPGETI/UFC – for travelling financial support that helped me to attend to a conference during my studies. Also, I am indebted to Fundação Cearense de Apoio ao Desenvolvimento Científico e Tecnológico – FUNCAP – for scholarship support.

To my mother Ana and my three sisters who pursue better opportunities inspired by my example. To my girlfriend Jéssica, who has given encouragement, support, advices and love in past years during my undergraduate and master studies.

ABSTRACT

THE infrastructure expansion planning in cellular networks, so called Base Station (BS) Placement (BSP) problem, is a challenging task that must consider a large set of aspects, and which cannot be expressed as a linear optimization function. The BSP is known to be a NP-hard problem unable to be solved by any deterministic method. Based on some fundamental assumptions of Long Term Evolution (LTE)-Advanced (LTE-A) networks, this work proceeds to investigate the use of two methods for BSP optimization task: the Particle Swarm Optimization (PSO) and the Differential Evolution (DE), which were adapted for placement of many new network nodes simultaneously. The optimization process follows two multi-objective functions used as fitness criteria for measuring the performance of each node and of the network. The optimization process is performed in three scenarios where one of them presents actual data collected from a real city. For each scenario, the fitness performance of both methods as well as the optimized points found by each technique are presented.

Keywords: Base Station Placement Problem, Particle Swarm Optimization, Differential Evolution

RESUMO

O planejamento de expansão de infraestrutura em redes celulares é uma desafio que exige considerar diversos aspectos que não podem ser separados em uma função de otimização linear. Tal problema de posicionamento de estações base é conhecido por ser do tipo *NP-hard*, que não pode ser resolvido por qualquer método determinístico. Assumindo características básicas da tecnologia *Long Term Evolution (LTE)-Advanced (LTE-A)*, este trabalho procede à investigação do uso de dois métodos para otimização de posicionamento de estações base: Otimização por Enxame de Partículas – *Particle Swarm Optimization (PSO)* – e Evolução Diferencial – *Differential Evolution (DE)* – adaptados para posicionamento de múltiplas estações base simultaneamente. O processo de otimização é orientado por dois tipos de funções custo com multiobjetivos, que medem o desempenho dos novos nós individualmente e de toda a rede coletivamente. A otimização é realizada em três cenários, dos quais um deles apresenta dados reais coletados de uma cidade. Para cada cenário, são exibidos o desempenho dos dois algoritmos em termos da melhoria na função objetivo e os pontos encontrados no processo de otimização por cada uma das técnicas.

Palavras-Chave: Problema de Posicionamento de Estações Base, Otimização por Enxame de Partículas, Evolução Diferencial

CONTENTS

List of Figures	11
List of Tables	12
Acronyms	13
Nomenclature	15
1 Introduction	18
1.1 Motivation	18
1.2 State of the Art	19
1.2.1 Network Planning Issues	20
1.2.2 Heuristics for Base Station (BS) Placement (BSP) optimization . . .	20
1.3 Objectives and Major Contributions	21
1.4 Thesis Organization	21
1.5 Scientific Production	22
2 Base Station Placement Modelling	23
2.1 Fundamentals	23
2.1.1 System Capacity	25
2.1.2 Base Station Load	26
2.2 Optimization Problem Formulation	26
2.2.1 Inserting New BSs	27
2.2.2 Runtime Analysis	28
2.3 Fitness Functions	29
2.3.1 Function 1: Network Index	29
2.3.2 Function 2: Capacity Maximization with Load Balancing	30
2.4 Summary of Base Station Placement Modelling	31
3 Spatial Optimization Techniques	32
3.1 Particle Swarm Optimization	32
3.1.1 Fundamentals	32
3.1.2 Mathematical Representation	33
3.1.3 Improvements in PSO topology	35
3.1.4 Simulation Chain	35
3.2 Differential Evolution Optimization	36
3.2.1 Fundamentals	36

3.2.2	Mathematical Representation	37
3.2.3	Simulation Chain	39
3.3	Summary of Optimization Techniques	39
4	System Model	40
4.1	Multi-cell Scenario	40
4.1.1	Grid Layout	40
4.1.2	Stochastic Geometry	40
4.1.3	Based on Real Data	41
4.2	UE Traffic Positioning and Representation	42
4.2.1	Randomly Heterogeneous User Equipments (UEs) Deployment . .	43
4.2.2	Grid UEs Deployment With Traffic Density	44
4.3	Simulation Cases	46
4.4	Fitness Functions	47
4.5	Environment Parameters	47
4.5.1	LTE Parameters	48
4.5.2	Traffic Model	49
4.6	Optimization Techniques Parameters	49
4.6.1	PSO Parameters	50
4.6.2	DE Parameters	50
4.7	Network Performance Metrics	51
4.8	Summary of System Model	51
5	Results	52
5.1	Case 1 – Grid layout	52
5.1.1	Fitness Function	52
5.1.2	Performance Results	54
5.1.3	Optimized Points	57
5.1.4	Summary of Optimization in Case 1	58
5.2	Case 2 – Stochastic Geometry	59
5.2.1	Performance Results	59
5.2.2	Network Performance Metrics	61
5.3	Case 3 – Real Data Based	65
6	Conclusion and Future Work	68
	References	69

LIST OF FIGURES

1.1	A multi-tier network composed with different kinds of cells	19
2.1	Network index functions	30
3.1	Update of individuals in PSO	34
3.2	Recombination process in DE	38
3.3	DE optimization process flowchart	38
3.4	Update of individuals in DE	38
4.1	Layouts for BS initial deployment regions	42
4.2	Variation of population density λ according to each neighbourhood	44
4.3	Traffic demand estimation and BS positions for City 1	45
4.4	Diagram of UEs deployment	46
5.1	Fitness functions φ in Grid layout	53
5.2	Cumulative Distribution Functions (CDFs) of number of iterations until find best solution in DE – Grid layout	55
5.3	PSO and DE performance for 8, 16 and 32 individuals – Grid layout	56
5.4	PSO performance – Fitness functions φ in Grid layout	57
5.5	DE performance – Fitness functions φ in Grid layout	58
5.6	CDFs of number of iterations until find best solution in DE when number of new BS = 1 – Stochastic Geometry layout	60
5.7	CDFs of number of iterations until find best solution in DE when number of new BS = 2 – Stochastic Geometry layout	60
5.8	PSO and DE fitness performance for 8 individuals placing 1, 2 and 4 new BSs – Stochastic Geometry	61
5.9	PSO and DE fitness performance for 16 individuals placing 1, 2 and 4 new BSs – Stochastic Geometry	62
5.10	PSO and DE fitness performance for 32 individuals placing 1, 2 and 4 new BSs – Stochastic Geometry	62
5.11	PSO and DE network performance for placing 4 new BSs with 8 and 16 individuals – Stochastic Geometry	63
5.12	PSO and DE network performance for 32 individuals placing 1, 2 and 4 new BSs – Stochastic Geometry	64
5.13	Fitness φ_2^* <i>versus</i> Iteration in Case 3	66
5.14	Capacity improvement <i>versus</i> Iteration in Case 3	67
5.15	Optimized points for deploying 8 new BSs using 128 PSO individuals	67

LIST OF TABLES

4.1	Large-scale fading model parameters for urban-micro environment	48
4.2	Large-scale fading model parameters for urban-macro environment	48
4.3	Parameters for LTE throughput (Simulation Cases 1 and 2)	49
4.4	Parameters for PSO optimization – Simulation Cases 1 and 2	50
4.5	Parameters for PSO optimization – Simulation Case 3	50
4.6	Parameters for DE optimization – Simulation Cases 1 and 2	50
5.1	Parameters for Simulation Case 1 – Grid Layout	52
5.2	Fitness results and best points found by PSO in 50 trials	54
5.3	Mean number of iterations until DE find best solution	54
5.4	Fitness results and best points found by DE in 50 trials	55
5.5	Parameters for Simulation Case 2 – Stochastic Geometry (SG) layout	59
5.6	Improvements on network metrics by optimization in SG layout – fitness function φ_2	65

ACRONYMS

1G	1 st Generation
2G	2 nd Generation
3G	3 rd Generation
3GPP	3rd Generation Partnership Project
4G	4 th Generation
5G	5 th Generation
AWGN	Additive white Gaussian noise
BS	Base Station
BSP	BS Placement
CDF	Cumulative Distribution Function
CoMP	Coordinated Multi-Point
dB	Decibel
DE	Differential Evolution
DL	Downlink
EE	Energy Efficiency
eNB	Evolved Node B
GA	Genetic Algorithm
GPS	Global Positioning System
HCPP	Hardcore Point Process
HetNet	Heterogeneous Network
ISD	Inter-site Distance
LOS	Line of Sight
LTE-A	LTE-Advanced
LTE	Long Term Evolution
MC-eNB	Macro-Cell Evolved Node B (eNB)
MIMO	Multiple-Input Multiple-Output
MMSE	Minimum Mean Square Error
mmW	Millimeter Wave
NLOS	Non-Line of Sight

NP-hard	Non-deterministic Polynomial-time hard
PC	Personal Computer
PC-eNB	Pico-Cell eNB
PCP	Poisson-cluster Process
PDF	Probability Density Function
PL	Path Loss
PPP	Poisson Point Process
PSO	Particle Swarm Optimization
QAM	Quadrature Amplitude Modulation
QoS	Quality of Service
RATs	Radio Access Technologies
SC-eNB	Small-Cell eNB
SG	Stochastic Geometry
SINR	Signal to Interference-plus-Noise Ratio
SISO	Single-Input Single-Output
SNR	Signal to Noise Ratio
UE	User Equipment
UL	Uplink

NOMENCLATURE

\mathbf{x}	Spatial position of UEs and BSs, page 23
PL	Path Loss, page 24
M_{UE}	Number of UEs, page 24
N_{BS}	Number of BSs, page 24
R	Distance between BS and UE (m), page 24
G^{TX}	Gain of transmitter antenna (dB), page 24
G^{RX}	Gain of receiver antenna (dB), page 24
p_{mn}	Received power (dBm), page 24
\mathbf{W}	Matrix of received power (dBm), page 24
\mathbf{w}_m	Received power of a single UE from all BSs (dBm), page 24
P^{TX}	Transmission Power (dBm), page 24
ψ	Received power from serving BS (dBm), page 24
$SINR$	Signal to Interference-plus-Noise Ratio (SINR) sensed by user (dB), page 25
N_0	Environment power noise (dBm), page 25
C	User capacity, page 25
BW	System Bandwidth, page 25
C^{total}	Sum of Capacities from all users, page 25
ℓ	Throughput limit for BS, page 25
τ	Maximum offered capacity for users, page 25
$load$	Traffic demand for BS, page 26
w^*	Received power inserting a new BS (dBm), page 27

L	Number of new BSs, page 28
S	Solution for the BSP problem, page 28
x	Ratio of BS load and maximum throughput, page 29
$N(x_n)$	Fitness function considering network ratio x , page 30
J	Jain's Index, page 31
M	Number of individuals for PSO and DE, page 32
x_i	Positions of PSO individuals, page 33
\vec{v}_i	Velocities of PSO individuals, page 33
x_i^*	Particle best PSO individual, page 33
x_g^*	Global best PSO individual, page 33
ϕ^*	Random perturbation in PSO update, page 34
c_{gB}	Acceleration coefficient for global best position in PSO, page 34
c_{pB}	Acceleration coefficient for individual best position in PSO, page 34
K	Number of iterations, page 35
\mathbf{v}_i	Donor vector in DE, page 37
\mathbf{x}_i	Target vector in DE, page 37
ζ	Crossover rate, page 37
\mathbf{u}_i	Trial vector in DE, page 37
ξ	Mutation factor, page 37
R_{earth}	Earth radius, page 41
λ	Density of points – Poisson processes, page 41
φ_i	Latitude, page 41
λ_i	Longitude, page 41
γ	Throughput demand, page 43

φ Fitness function for optimization, page 47

P_{min} Fitness function for optimization, page 51

1. INTRODUCTION

THIS chapter introduces the main motivations of this work in Section 1.1 followed by a review of the state of the art of the BSP problem in Section 1.2, where I present the evolution of network planning strategies. I list the objectives, major contributions of this work and thesis organization in Sections 1.3 and 1.4, respectively. Finally I present my scientific production during the master course in Section 1.5.

1.1 Motivation

The continuous development of wireless communications systems, since early generations to advanced technologies, has made possible the growth of such volume of mobile services hard to be imagined half a century ago. Thanks to the development of Electronics and Telecommunications Engineering in the past 40 years, with the exponential growing of electronic hardware computational power and more efficient usage of wired and wireless channels, it seems there is no boundaries for the worldwide, personal and efficient mobile communications, allowing people to be in contact with each other effortlessly.

However, as new mobile communication services become available, the usage of these services begin to grow rapidly. Recently, the amount of Internet accesses from smartphones and tablets considering only mobile applications overtook Personal Computers (PCs) Internet usage in the United States [1]. The increase of smartphone usage is expected to be about 35% per year [2], but there is a question: are the operators ready to support this growing with current technology?

For next wireless networks generations, i.e., 5G, wireless networks are expected to be a mixture of network tiers of different sizes, transmit powers, backhaul connections, several Radio Access Technologies (RATs) that are accessed by an unprecedented number of smart and heterogeneous wireless devices [3]. Thus, the heterogeneity and increasing number of network nodes, shown in Figure 1.1, will make it difficult to perform infrastructure planning.

In order to make users able to appreciate these possibilities, operators must attain major keys of current mobile technology specifications, the Long Term Evolution (LTE), by providing acceptable data rates and latency for satisfying their experience. Indeed, the main way of guaranteeing network quality is setting up a good infrastructure by adjusting both the amount and position of network nodes close to regions with large number of subscribers or services' demand. Nevertheless, the arrangement of infrastructure is one of

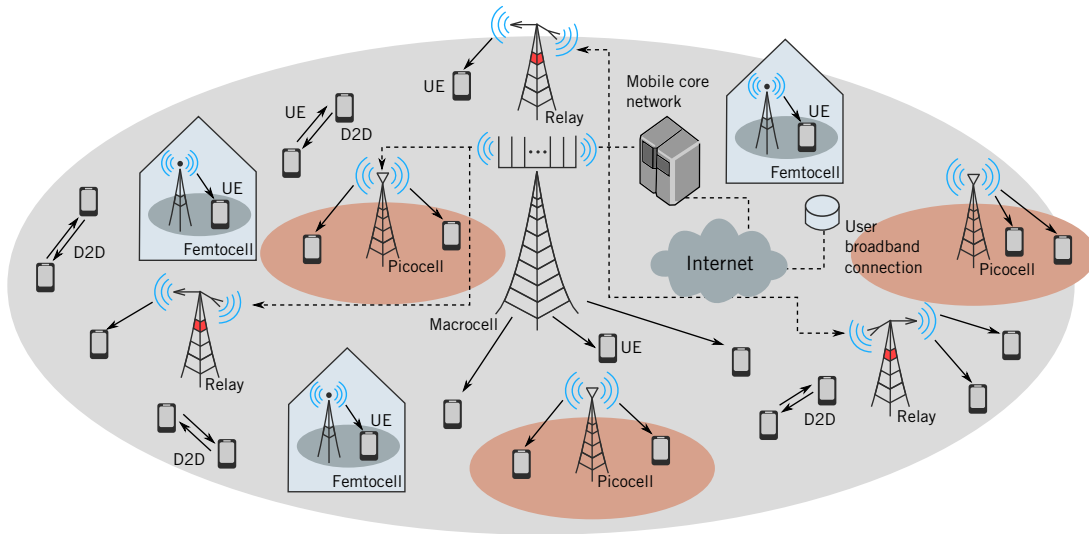


Figure 1.1: A multi-tier network composed with different kinds of cells

the most important design tasks because it represents capital expenditure for operators, so that ideally it must be done as to improve user's satisfaction proportionally. There is still room for studying the BS Placement (BSP) problem because each mobile communications generation proposes different set points of requirements.

1.2 State of the Art

In early wireless network generations, it was established the radio planning had to start from the predictions of coverage to estimate the number of base stations to cover a given area [4], so 1st Generation (1G) and 2nd Generation (2G) planning design were more oriented to coverage, but with the evolution of mobile technologies the rapidly growing usage of broadband made the data rates experienced by the users in the network become increasingly important [5], i. e., the infrastructure expansion planning in 3rd Generation (3G) was more oriented to capacity, leading to high throughput. The paradigm for 4th Generation (4G) cellular networks was lead towards a high-data rate, low-latency and packet-optimized radio access technology [6], resulting in an improvement of experienced data-rates by two and three times on Uplink (UL) and Downlink (DL), respectively compared to the previous generation and the use of flat architecture with radio-related functionalities located in the BS [7]. This results in attainment of multiple services with demanding data-rates, such as high quality video streaming for mobile devices. Finally, besides improvement on data rates, it is expected an alignment for 5th Generation (5G) networks with Energy Efficiency (EE).

From the operator's perspective, the network deployment process is the first step they have to face when supplying a set of services to their customers [8]. In order to

attain success in the market, operators normally use strategic and operative software tools for designing, planning and optimizing wireless networks, which are money-savers for their business. Nevertheless, while operators keep providing wireless access services, the technologies change demands repetition of network planning tasks based on new requirements. Thus, it is very common to observe two or three different technologies supported by an operator at the same time in order to satisfy many users' requirements simultaneously. Finally, the plan of deploying LTE 4G networks to satisfy the increasing of traffic demands translates into a continuous need for LTE cell sites planning [9].

1.2.1 Network Planning Issues

The BSP optimization task depends on a set of variables, such as traffic density, channel condition, interference scenario, number of BSs, etc. [10] defines the cell planning problem as searching for a subset of base stations' positions $\{BS^o\} \subseteq \{BS^*\}$ that satisfies desired criteria, where $\{BS^*\}$ corresponds to all possible configurations for BSs. Because of the relation and combination between these variables, BSP is an Non-deterministic Polynomial-time hard (NP-hard) problem [11] for which it is not possible to find a polynomial time algorithm in the theory of computational complexity. Instead of performing exhaustive combination of all possibilities as solution of this problem, many works suggested strategies using specially evolutionary and heuristic algorithms. A general optimization algorithm is implemented to optimize BS placement in a very realistic scenario containing a large set of variables. However, this large number of attributes makes algorithms' runtime very long. On the other hand, limiting the set of variables produces coarse results. Furthermore, the optimization problem can be formulated with various objectives, for example: capacity enhancement, network lifetime maximization, power and node number minimization [12].

1.2.2 Heuristics for BSP optimization

Some applicable heuristic methods for the BSP problem are described below:

- **Particle Swarm Optimization (PSO):** It was introduced by [13] in 1995 as an optimization method for continuous non-linear functions and it inspired in social psychological principles of the behaviour of bird flocks under foraging process. This optimization method was applied for the BSP problem in several works: in [14] the authors deployed BSs to maximize coverage and economy efficiency obtaining 91.12% of coverage after 100 iterations; the work of [15] aimed at capacity maximization and network balancing assuming a soft handover mechanism. On its turn, [16] focused on the optimization of Coordinated Multi-Point (CoMP) antenna ports regarding

various UE distribution. These works considered network planning for the first placement of BSs. PSO has also been tested on wireless network optimization, such as sensor's coverage [17].

- **Differential Evolution (DE):** It was presented to scientific community by the year of 1995 in the First International Competition on Evolutionary Optimization by Price and Storn [18]. The strength of the algorithm lies in its simplicity, speed and robustness [19]. Also, DE was verified in wireless sensors network optimization in [20] with the goal of finding the best operational mode for each sensor in order to minimize energy consumption.

1.3 Objectives and Major Contributions

The objectives of this work are described as follows:

- Present the BSP task as an optimization problem;
- Adapt PSO and DE to the BSP problem for the placement of a single or multiple bases and evaluate their performance by measuring their fitness;
- Apply these heuristic methods in a real-based scenario consisting on real information of BSs' position and traffic estimates derived from population data;

As main contribution, this work validates the use of PSO and DE as suitable techniques for BSP optimization. The specific objectives are:

- Definition of fitness functions for optimization process based on network aspects in Chapter 2;
- Modelling of many wireless network scenarios in Chapter 4;
- Compare PSO and DE performance for those layouts in Chapter 5.

1.4 Thesis Organization

This thesis is organized as follows: Chapter 2 discusses the fundamentals of BSP modelling, formulates the task of placing one or multiple BSs as an optimization problem and defines a set of fitness functions used to measure performance of heuristic methods. Chapter 3 shows the mathematical fundamentals of PSO and DE, presenting their main characteristics. In Chapter 4 the system modelling is described, with definition of which scenarios are used, how UEs are represented and how to construct a real-based scenario. The presentation and discussion of numerical simulation results using these heuristics is

shown in Chapter 5 for all scenarios described previously in Chapter 4. The summary of simulation results and further expectations of this work is exhibited in Chapter 6.

1.5 Scientific Production

The following work was submitted and accepted for a conference during the Master period.

- **M. B. Pereira**, F. R. P. Cavalcanti, and T. F. Maciel, "Particle swarm optimization for base station placement," in *International Telecommunications Symposium*, Aug 2014.

2. BASE STATION PLACEMENT MODELLING

EVALUATING the BSP optimization problem requires mathematical modelling in order to verify the practicability of obtaining an exact solution using a close expression or either applying an optimization technique. This chapter exhibits mathematical development for modelling this problem regarding a region composed of sets of BSs and UEs with two dimensional positions.

2.1 Fundamentals

Wireless propagation radio channels confront several issues. In fact, the wireless signals suffer severe attenuation in links between BSs and UEs caused by dissipation of the power radiated by the transmitter as well as effects of the propagation channel. The modelling of attenuation on received signal strength in the receptor can be assumed as *physical* or *statistic*: the second one takes empirical approaches, measuring propagation characteristics in a variety of domains and developing these models for a class of particular environments [21]. From these statistical representations, attenuation depends on many parameters which can be split in two parts: the *path loss* and *shadowing*, described below:

- *Path Loss (PL)* is the ratio of transmitted p_T and received p_R power, which can be given in linear scale or in Decibel (dB) scale (2.1):

$$PL = \frac{p_T}{p_R} \quad \rightarrow \quad PL_{\text{dB}} = 10\log_{10}PL \text{ dB.} \quad (2.1)$$

Because most mobile communication systems operate in complex propagation environments that cannot be accurately modelled by free-space path loss or ray tracing, many path loss models have been developed over the years [22] to predicting channel effects in many environments. These theoretical and measurement-based propagation models indicate that average received signal strength decreases with the distance R between transmitter and receiver [23]. The value of R depends on the absolute distance between spatial positions from sets of M UEs and N BSs, where each UE_m and BS_n contain spatial positions represented by $UE_m(\mathbf{x})$ and $BS_n(\mathbf{x})$, respectively, such that $\mathbf{x} = [x_1 \ x_2]$ in a two-dimensional plane. The distance between these nodes is given by R_{mn} , which denotes their absolute distance as shown in (2.2):

$$R_{mn} = |UE_m(\mathbf{x}) - BS_n(\mathbf{x})|. \quad (2.2)$$

Given an empirical *pathloss* model and the distance R_{mn} between each UE_m and BS_n , the PL_{mn} can be obtained by any general expression (2.3):

$$PL_{mn} = \text{pathloss}(R_{mn}). \quad (2.3)$$

- *Shadowing* (χ) is caused by obstacles between the transmitter and receiver that attenuate signal power through absorption, reflection, scattering, and diffraction [22]. This effect was also verified empirically and is often modelled as a log-normal random variable with mean μ_χ and standard deviation σ_χ , defined for each empirical scenario.

Eventually, experimental models depend on definitions of the environment characteristics, such as BS antenna heights, average building height, distance between buildings, etc. Such information will be detailed in Chapter 4.

Considering the downlink scenario, the BSs and UEs are the transmitter and receiver nodes, respectively, from which each BS_n has transmission power P_n^{TX} , or P_n^{BS} . Also, other attributes are defined for downlink case in order to model the links between BSs and UEs, such as *antenna gains* for transmitter G_n^{TX} , or G_n^{BS} , and receiver G_m^{RX} , or G_m^{UE} , given in dB, which depend on the radiation pattern of these antennas. With possession of these attributes, the received power p_{mn} at the UE_m from BS_n is estimated by:

$$p_{mn} = P_n^{BS} + G_m^{BS} + G_n^{UE} - PL_{mn} + \chi_{mn}. \quad (2.4)$$

From received power values, p_{mn} , the matrix \mathbf{W} presents signal strengths from all links between UEs and BSs (2.5):

$$\mathbf{W} = \begin{bmatrix} p_{11} & p_{12} & \cdots & p_{1N} \\ p_{21} & p_{22} & \cdots & p_{2N} \\ \vdots & \vdots & \ddots & \vdots \\ p_{M1} & p_{M2} & \cdots & p_{MN} \end{bmatrix} = \begin{bmatrix} \mathbf{w}_1 \\ \mathbf{w}_2 \\ \vdots \\ \mathbf{w}_M \end{bmatrix}, \quad (2.5)$$

where row vectors $\mathbf{w}_m = [p_{m1} \ p_{m2} \ \cdots \ p_{mN}]$ collect the received powers for UE_m from all BSs.

The highest value in each vector \mathbf{w}_m is the maximum received power for UE_m . Assuming the maximum received signal strength corresponding to power received from the serving BS, the other values in \mathbf{w}_m are interpreted as interfering signals from all remaining bases. Considering the following statement:

$$\psi_m = \max(p_{m1}, p_{m2}, \cdots, p_{mN}),$$

$$\psi_m = \max(\mathbf{w}_m), \quad (2.6)$$

if each BS uses all network spectrum resources and all links between BSs and UEs are assumed as active in the network, the SINR is obtained as follows (2.7), given ψ_m and \mathbf{w}_m converted from dB to linear scale:

$$SINR_m = \frac{\psi_m}{\sum_{n=1}^N p_{mn} - \psi_m + N_0}, \quad (2.7)$$

where N_0 denotes the Additive white Gaussian noise (AWGN) power noise. The expression $\sum_{n=1}^N p_{mn} - \psi_m$ is the sum of the powers received from all BSs minus the power incoming from the serving BS, thus resulting in the sum of the interference contributions, since the network model assumes a fully loaded system, in which all links are active. Finally, from Shannon equation [24], the capacity C for this configuration is denoted by:

$$C_m = BW \cdot \log_2(1 + SINR_m) \text{ bps}, \quad (2.8)$$

where BW denotes system bandwidth. A general expression assumes $BW = 1$ and returns capacity in bits per second per Hertz (bps/Hz).

2.1.1 System Capacity

The capacity shown previously (2.8) is evaluated for a single user under the propagation characteristics described in Section 2.1. Supposing the network has fully loaded links between UEs and BSs, which are presumed to potentially serve all these users in its full demand, the theoretical total capacity that could be sensed by users is interpreted as the sum of single capacities for UEs (2.9):

$$C^{total} = \sum_{m=1}^M C_m. \quad (2.9)$$

Although the amount of capacity sensed by users considers only their SINRs (2.8), in a multicellular scenario the BSs have a maximum traffic which can be offered to connected UEs. It means that the provided capacity for users is limited by the sum of the maximum allowed traffic of all BSs. Assuming each BS has a throughput limit of ℓ_n , the maximum capacity τ offered for users becomes:

$$\tau = \sum_{n=1}^N \ell_n. \quad (2.10)$$

Thus, the total offered capacity τ might be higher or lower than the sum of sensed capacities C^{total} depending on the network planning. The choice of traffic model impacts on the network evaluation by means of BSs overload. Adopting a full buffer traffic characterized by a fixed number of users in the cell and the buffers of the users' data flows always having unlimited amount of data to transmit/receive [25] require full dimensioning of users' demand.

2.1.2 Base Station Load

The measurement of BSs' load depends on the amount of traffic demanded by each BS, associating users with bases that provide the strongest power for them. From (2.6), the maximum value of w_m is equivalent to its received power, therefore, the position where the highest value is found corresponds to the index of BS that services the UE_m .

Considering the subset of M^* UEs as $\{UE_1, UE_2, \dots, UE_{M^*}\}_n$ that are connected only to BS_n and assuming their capacities as $\{C_1, C_2, \dots, C_{M^*}\}_n$, the expected load for a single BS is:

$$load_n = \sum_{m=1}^{M^*} C_m. \quad (2.11)$$

The measurements on the BS load capture a more specific characteristic of network in terms of BSs' overload. For example, the offered capacity, τ , can be equal to users' demand, C^{total} , but existing any BS, BS_n , where the load $load_n$ is higher than its offered throughput, ℓ_n . From the evaluation of BSs loads, a measurement of overload of bases can be asserted and regions where users are affected by high traffic load can be mapped.

2.2 Optimization Problem Formulation

The *optimization problem* consists of finding a solution with either maximum or minimum measurement [26] for a fitness or objective function. A mathematical optimization problem has the following form [27]:

$$\begin{aligned} & \text{minimize} && f_0(\mathbf{x}) \\ & \text{subject to} && f_i(\mathbf{x}) \leq b_i, \quad i = 1, \dots, m. \end{aligned} \quad (2.12)$$

The vector \mathbf{x} corresponds to the *optimization variable* and the function $f_0 : \mathbb{R}^N \rightarrow \mathbb{R}$ is the *objective function*, the functions $f_i : \mathbb{R}^N \rightarrow \mathbb{R}$ are *constraint functions* and b_1, \dots, b_m correspond to limits for constraints.

As mentioned earlier the BSP placement problem is known to be Non-deterministic

Polynomial-time hard (NP-hard), which cannot be solved by algorithms in polynomial time. Furthermore, if objective or constraint functions are not linear and not known to be convex, the general non-linear programming problem shown in (2.12) requires alternative optimization algorithms, which is the case of capacity-based objective functions.

2.2.1 Inserting New BSs

The problem formulation starts by modelling the positioning of a new BS in the environment. Rewriting the received power matrix (2.5) when inserting one new BS as:

$$\mathbf{W} = \left[\begin{array}{cccc|c} p_{11} & p_{12} & \cdots & p_{1N} & p_{1N+1} \\ p_{21} & p_{22} & \cdots & p_{2N} & p_{2N+1} \\ \vdots & \vdots & \ddots & \vdots & \vdots \\ p_{M1} & p_{M2} & \cdots & p_{MN} & p_{MN+1} \end{array} \right] = \left[\begin{array}{c|c} \mathbf{w}_1 & p_{1N+1} \\ \mathbf{w}_2 & p_{2N+1} \\ \vdots & \vdots \\ \mathbf{w}_M & p_{MN+1} \end{array} \right] = \left[\begin{array}{c} \mathbf{w}_1^* \\ \mathbf{w}_2^* \\ \vdots \\ \mathbf{w}_M^* \end{array} \right], \quad (2.13)$$

where the column $N + 1$ contains powers obtained when setting a single new BS. The expressions for SINR and capacity shown in (2.7) and (2.8) differ only in the ψ value due to the changing on the interference originated from inserting new bases. The maximum received power ψ_m from (2.6) becomes:

$$\begin{aligned} \psi_m^* &= \max(p_{m1}, p_{m2}, \dots, p_{mN}, p_{m,N+1}), \\ \psi_m^* &= \max(\mathbf{w}_m^*). \end{aligned} \quad (2.14)$$

Although the placement of a new base $N + 1$ increases total offered throughput by $\tau + \ell_{N+1}$, the users' sensed sum of capacities would increase or diminish due to interference effects.

When using capacity-based functions as fitness, the optimization problem is NP-hard, since the individual users' capacities (2.11) depends on the SINRs, which is a non-linear function of BS' positions \mathbf{x} . The placement of a single new BS can determine an approximate optimal position \mathbf{x} *a priori* by using one of the following methods:

- **Exhaustive Search** by disposing random points in the map and test each one on the fitness function, for which precision varies with the number of trials for finding minimum or maximum.
- **Grid Method** by creating a grid set of points and testing all of them. The precision depends on the length of data set, i.e., on the grid spatial resolution.

Due to the fact of the precision of both methods relies on the quantity of tested points, the number of trials for finding the solution may be enormous. Depending of the

size of the search space and the desirable precision, the solution can be obtained with a good accuracy with relatively low number of tests, e.g., thousands of points.

Now assuming the placement of L new bases, (2.13) can be rewritten considering multiple BSs as shown below:

$$\begin{aligned} \mathbf{W} &= \left[\begin{array}{cccc|ccc} p_{11} & p_{12} & \cdots & p_{1N} & p_{1N+1} & \cdots & p_{1N+L} \\ p_{21} & p_{22} & \cdots & p_{2N} & p_{2N+1} & \cdots & p_{2N+L} \\ \vdots & \vdots & \ddots & \vdots & \vdots & \ddots & \vdots \\ p_{M,1} & p_{M2} & \cdots & p_{MN} & p_{MN+1} & \cdots & p_{MN+L} \end{array} \right] \\ &= \left[\begin{array}{c|ccc} \mathbf{w}_1 & p_{1N+1} & \cdots & p_{1N+L} \\ \mathbf{w}_2 & p_{2N+1} & \cdots & p_{2N+L} \\ \vdots & \vdots & \ddots & \vdots \\ \mathbf{w}_M & p_{MN+1} & \cdots & p_{MN+L} \end{array} \right] = \left[\begin{array}{c} \mathbf{w}_1^* \\ \mathbf{w}_2^* \\ \vdots \\ \mathbf{w}_M^* \end{array} \right]. \end{aligned} \quad (2.15)$$

The placement of L new BSs will increase the offered throughput to $\tau + \sum_{l=1}^L \ell_{N+l}$, corresponding to a potentially substantial improvement on the network throughput. On the other hand, the amount of interference $\sum_{m=1}^{N+L} p_{mm} - \psi_m$ will be greater, causing the users' sensed capacity to be lower, thus decreasing the Quality of Service (QoS) of network.

In the case of placing L new bases, the search for nearly optimal solutions increases exponentially with L , because it is necessary to test every combination of L possible new solutions.

2.2.2 Runtime Analysis

Consider both approximate methods for searching optimal points described in 2.2.1 and ignoring the complexity of evaluating the fitness function, assume that finding the optimal position for inserting one single base requires testing K candidate positions. Now, assuming $S(1)$ as the solution for placing this one new base, consider as true the following statement:

$$S(1) \supseteq \{\mathbf{x}_1\}. \quad (2.16)$$

Then, expanding this solution to place L bases leads to:

$$\begin{aligned} S(2) &\supseteq \{\mathbf{x}_1, \mathbf{x}_2\} \\ S(3) &\supseteq \{\mathbf{x}_1, \mathbf{x}_2, \mathbf{x}_3\} \\ &\vdots \\ S(L) &\supseteq \{\mathbf{x}_1, \mathbf{x}_2, \cdots, \mathbf{x}_L\}. \end{aligned} \quad (2.17)$$

Since the first solution $S(1)$ is obtained after testing K points, the search of solution $S(L)$ requires testing K^L sets of points to find the solution $[\mathbf{x}_1 \ \mathbf{x}_2 \ \cdots \ \mathbf{x}_L]$. Depending on the calculation time for measuring fitness, this growing of the number of required operations makes it difficult to use the exhaustive search technique. Moreover, due to the fact that variations in the set of positions for BSs affect the SINR values, the optimal points might be different for any solution.

2.3 Fitness Functions

Fitness functions are used to compare different solution sets or make optimization processes converge to a global value. The fitness functions are composed by some objective criteria that evaluate the performance of: 1) only new BSs or 2) the entire network. The combination of measurements on demanded capacity of users C^{total} and overload of bases $load_n$ results into the definition of our fitness functions: the *Network Index*, which aims to maximize performance of BSs without overloading them, and the *capacity maximization with load balancing*, whose objective is balancing BSs load and maximizing users' sensed capacity simultaneously. These fitness functions are described in following subsections.

2.3.1 Function 1: Network Index

Assuming each BS has a maximum throughput ℓ_n , the amount of resources that can be shared for all connected UE will be limited even if the sum of capacities of users is greater than BS maximum throughput. The metric called *network ratio* x_n defined here establishes a factor to measure the overload of BS and it equals the ratio between the BS load described in (2.11) and its throughput limit ℓ_n (2.18):

$$x_n = \frac{\sum_{m=1}^{M^*} C_m}{\ell_n},$$

$$x_n = \frac{load_n}{\ell_n}. \quad (2.18)$$

Based on the domain of variable $x_n \in [0, \infty)$, let us make the following assessments:

- **Case 1:** When $x_n < 1$, the sum of throughputs of users is lower than the BS's throughput maximum, thus, the requirements of users will be fully served, but the base has not been demanded on its limit yet;
- **Case 2:** If $x_n > 1$, the capacity demand from all UEs is higher than the BS's throughput maximum, hence, some users will experience a lack in the fulfilment of their

demands;

- **Case 3:** In the case of $x_n = 1$, the BS has assigned all its capacity for all users, fulfilling their requirements.

For a wireless network, the aim is the optimization of positions for nodes in order to make each BS close to **case 3** operation because the amount of available resources is equal to users' demands. Thus, the objective function must map x_n so resulting on its highest value when **case 3** is achieved. Defining $N(x_n)$ as objective function, it is designed to have image $N(x) \in [0, 1]$, with maximum at $x = 1$ and minimum at 0 and ∞ in order to focus optimization towards **case 3**. Moreover, the mapping of these cases to fitness values results in the continuous function $\eta_1 = N(x_n)$ suitable to represent the effects of overload as:

$$N(x_n) = x_n^\alpha \cdot e^{(1-x_n^\alpha)}, \quad \alpha \in \mathbb{R} : \alpha \geq 2. \quad (2.19)$$

Figure 2.1 exhibits the network index functions (2.19) emphasizing that the variation of α parameters affects the sensitiveness for very low or large values of x . The fitness function has no unity for its values.

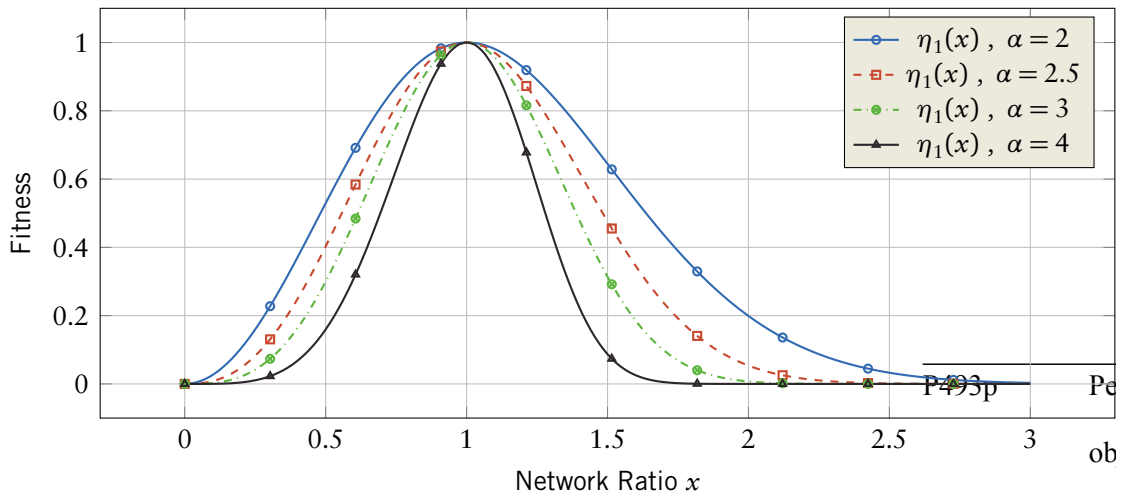


Figure 2.1: Network index functions

2.3.2 Function 2: Capacity Maximization with Load Balancing

The *capacity maximization with load balancing* metric targets the increase of the mean throughput of all users, based on total capacity, C^{total} , (2.9), while balancing the BSs load, $load_n$, (2.11).

The distribution of demands in all network BSs is based on the quantitative concept of fairness measurement proposed by Jain [28], which estimates distribution of resources in a system. From all N BSs load, considering $load_n$ as the shared resource, the *Jain's*

Index J for BSs loads (2.20) is given as:

$$J = \frac{\left(\sum_{n=1}^N load_n\right)^2}{N \cdot \left(\sum_{n=1}^N load_n^2\right)}. \quad (2.20)$$

The variable $load_n \in [0, \infty]$ results in $J \in [1/N, 1]$. Moreover, the value $J = 1$ means that all BSs have the same load demand.

Now supposing the set of M UEs which has mean throughput equals to:

$$\bar{C} = \frac{C^{total}}{M}, \quad (2.21)$$

thus, combining the J value with the users total throughput mean demand \bar{C} (2.22):

$$\eta_2 = J \cdot \bar{C}. \quad (2.22)$$

2.4 Summary of Base Station Placement Modelling

This chapter described major aspects used in this work for performing the optimization process on the BSP problem, such as the difficulty to find solutions because of the inherent problem complexity. Also, it exhibited two fitness functions which measure single BS and network performance. The following Chapter 3 presents two heuristic methods for BSP optimization.

3. SPATIAL OPTIMIZATION TECHNIQUES

MANY optimization problems focus on maximization or minimization of fitness functions, but the optimization using classical approaches may be onerous if the search space of the utility function is hard to be modelled mathematically. As discussed in Section 2.2.1, for the BSP problem, each new point inserted in the search space affects the overall performance parameters for all network nodes. Even for finding a nearly optimal solution, this NP-hard problem requires an exhaustive combinatorial search, which makes the simulation time grow very quickly depending of the number of BS positions for combination.

Under these conditions, some heuristic-based methods for finding nearly-optimal solutions might be considered, since they present good results without a very high computational cost.

This chapter presents two methods of finding good near optimal solutions: Particle Swarm Optimization (PSO) and the Differential Evolution (DE), both inspired by biological and sociological motivations and able to take care of optimality on rough, discontinuous and multi-modal surfaces [19].

3.1 Particle Swarm Optimization

3.1.1 Fundamentals

The Particle Swarm Optimization (PSO) is a population-based stochastic algorithm for optimization inspired by social-psychological principles [29]. PSO differs from other evolutionary algorithms because it uses all population members from the beginning of a trial until its end. The principle of PSO is based on the idea that these population individuals move within the solution space influencing each other with stochastic changes, while previous successful solutions act as attractors [30]. Thus, the interactions of individuals with each other result in incremental improvement of the quality of problem solutions over time.

In PSO a set of M simple entities, also called *particles*, are placed in the search space of some problem. Each particle evaluates the objective function – the *fitness* – at the current location or particles for each iteration. Their movements are given by a velocity vector \vec{v} calculated for each particle using a combination of two attributes: *social*

influence and *persistence*; and considering some random perturbation.

3.1.2 Mathematical Representation

When representing problem in a \mathbb{R}^2 space, each particle P_i in PSO contains two vectors with same dimension as the search space. The position of particle is represented by a vector x_i (3.1a) while its velocity is represented by \vec{v}_i (3.1b); both attributes relates to the same iteration k . Given current position and velocity of a particle, PSO performs the movement of individuals by updating position with $x_i[k+1]$ in the next iteration $k+1$ obtained by adding current $x_i[k]$ and $\vec{v}_i[k]$ in iteration k (3.2):

$$P_i \begin{cases} x_i = [x_1 \ x_2]_i, & (3.1a) \\ \vec{v}_i = [v_1 \ v_2]_i, & (3.1b) \end{cases}$$

$$x_i[k+1] = x_i[k] + \vec{v}_i[k]. \quad (3.2)$$

Assuming a random deployment of individuals and a random selection of their velocities as initial conditions, the update of positions and velocities depends on the behaviour of particles regarding the fitness function within the search space. Two major factors affect the optimization process:

- **Persistence**, which considers the best position reached by a single individual P_i , the *best particle* represented by x_i^* . The persistence on the particle P_i is:

$$persistence = (x_i^* - x_i[k]),$$

thus, this parameter measures how far is the position of P_i to the best position found by PSO;

- **Social Influence**, which relates to the best position ever found by the entire set of particles, called also *global best* and represented as x_g^* . The social influence on particle P_i is represented by:

$$social\ influence = (x_g^* - x_i[k]),$$

so this attribute calculates distance of the position of P_i and the best position ever found by the group of particles.

Considering these two factors described above, PSO updates the velocity parameter in each iteration, as shown in (3.3). Both social influence and persistence attributes are scaled by two parameters: ϕ_i^* for individual contribution and ϕ_g^* for global contribution.

Thus, one has

$$\vec{v}_i[k+1] = \vec{v}_i[k] + \phi_i^* \cdot (x_i^* - x_i[k]) + \phi_g^* \cdot (x_g^* - x_i[k]). \quad (3.3)$$

Moreover, (3.3) can be verbally read as:

$$\text{NEW VELOCITY} = \text{CURRENT VELOCITY} + \text{PERSISTENCE} + \text{SOCIAL INFLUENCE}. \quad (3.4)$$

Therefore, the update of positions assumes new velocities obtained in every optimization iteration.

The ϕ_i^* and ϕ_g^* parameters determine the strength of random perturbations towards global and individual best positions $P_i^{*ind} \in P^{*global}$ [31], also called *acceleration coefficients*. Each of these perturbations can be rewritten as a product of the form $\phi^* = c \cdot \phi$, where c is a known scalar and ϕ is a uniform random variable between 0 and 1. Each influence attribute is scaled with constants c_{pB} and c_{gB} , respectively. The update of velocity in (3.5) is represented by:

$$\vec{v}_i[k+1] = v_i[k] + c_{pB} \cdot \phi_i \cdot (x_i^* - x_i[k]) + c_{gB} \cdot \phi_g \cdot (x_g^* - x_i[k]). \quad (3.5)$$

The effect of individuals update in PSO for a 2-dimensional search space is shown in Figure 3.1.

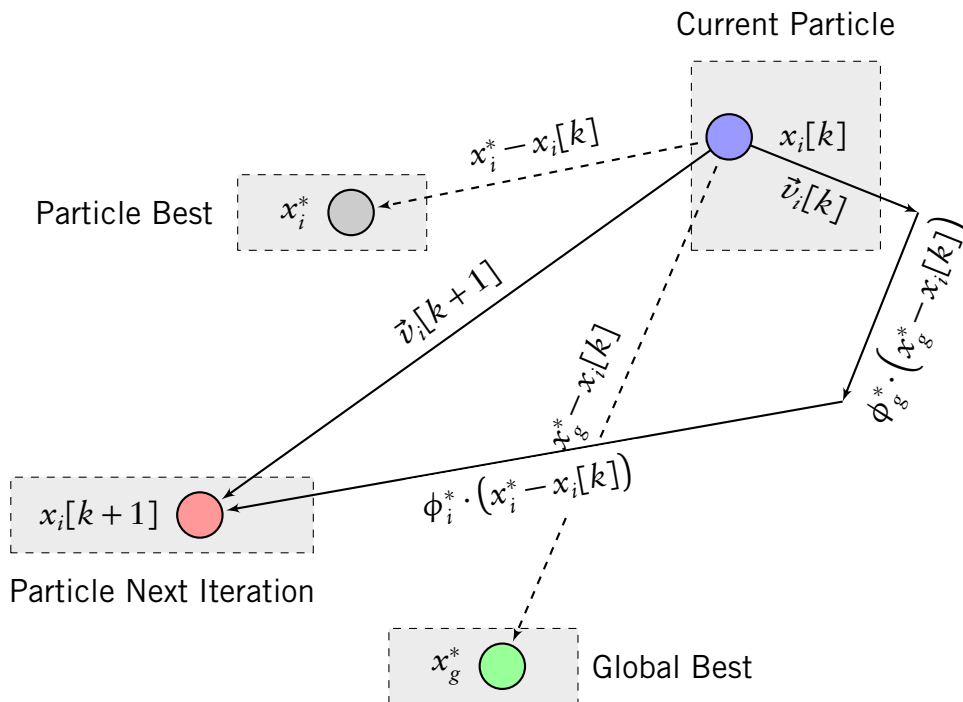


Figure 3.1: Update of individuals in PSO

3.1.3 Improvements in PSO topology

Some studies proposed improvements in PSO by including an inertia weight for velocities and updating both social influence and persistence parameters, as shown below:

1. **Inertia coefficient:** As proposed in [32], the inclusion of a decreasing coefficient for velocities' update is effective for reducing the inertia of the particles. This characteristic stabilizes the position of individuals in late iterations. Assuming K iterations, and given initial w_0 and final w_K values for inertia, $w[k]$ for each iteration k are equal to:

$$w[k] = w_0 + \frac{k}{K} \cdot (w_K - w_0). \quad (3.6)$$

That variation in inertia coefficient affects *exploration*, when individuals are lead to search towards new unexplored regions, and *exploitation*, when they take advantage of positions where good fitness values were found previously.

2. **Variation in Social Influence and Persistence:** The work of [33] assumes also a temporal variation for social and individual attributes, c_{gB} and c_{pB} . This concept emphasizes local or global search in different periods of optimization, similar to the idea of variation in acceleration discussed previously. Given initial and final values for c_{gB} and c_{pB} as $\{c_0, c_K\}$, the variation of both coefficients is performed by:

$$c[k] = c_0 + \frac{k}{K} \cdot (c_K - c_0). \quad (3.7)$$

Regarding these two improvements, a general update for velocities in PSO becomes:

$$\vec{v}_i[k+1] = w[k] \cdot \vec{v}_i[k] + c_{pB}[k] \cdot \phi_i \cdot (x_i^* - x_i[k]) + c_{gB}[k] \cdot \phi_g \cdot (x_g^* - x_i[k]). \quad (3.8)$$

3.1.4 Simulation Chain

A generic simulation chain for the PSO algorithm is shown in Algorithm 1 present the optimization process considering the particles' positions x_i and velocities v_i lead by a fitness function η , which should be maximized or minimized (\gtrless). The optimization algorithm requires input parameters such as acceleration coefficients w_0 and w_K , if they present variation, and in constants c_{pB} and c_{gB} .

Algorithm 1 PSO algorithm

```

1: Set up initially  $M$  particles  $P_i, i = 1, \dots, M$ 
2: Define  $w_0, w_K, c_{pB}$  and  $c_{gB}$ 
3: for all Particles  $P_i$  do
4:   Set  $x_i$  and  $v_i$ 
5: end for
6: Set  $P^{*ind} \leftarrow P_1$  and  $P^{*global} \leftarrow P_1$ 
7: for  $K$  iterations do
8:   Compute acceleration  $w_k \leftarrow w_0 + (k/K) \cdot (w_K - w_0)$  (3.6)
9:   for all Particles  $P_i$  do
10:    compute fitness  $\eta_i, \eta^{*ind}$  and  $\eta^{*global}$  for  $P_i, P^{*ind}$  and  $P^{*global}$ 
11:    if  $\eta_i \geq \eta^{*ind}$  then
12:       $P^{*ind} \leftarrow P_i$ 
13:    end if
14:    if  $\eta_i \geq \eta^{*global}$  then
15:       $P^{*global} \leftarrow P_i$ 
16:    end if
17:     $persistence \leftarrow \phi \cdot (P_i - P^{*ind})$ 
18:     $social\ influence \leftarrow \phi \cdot (P_i - P^{*global})$ 
19:     $\vec{v}_i \leftarrow w_k \cdot \vec{v}_i + c_{pB} \cdot persistence + c_{gB} \cdot social\ influence$  (3.8)
20:     $x_i \leftarrow x_i + \vec{v}_i$  (3.2)
21:   end for
22: end for

```

3.2 Differential Evolution Optimization

3.2.1 Fundamentals

Differential Evolution (DE) is a stochastic parallel search method for maximization or minimization of fitness functions [34]. DE was originally designed to handle optimization of real-valued functions based specially on the use of a differential operator to create new individuals for following generations, which is an advantage compared to the classical Genetic Algorithm (GA), designed for discrete search spaces.

This technique performs a parallel search in a N -dimensional region using M single entities, with the same dimension of the search space, as population for each generation k , attempting to replace all points in search space S by new positions at each generation [35]. A general formulation for optimization of the DE-based is to find \mathbf{x}^* given the objective function $f: \mathbf{X} \subseteq \mathbb{R}^N \rightarrow \mathbb{R}$, i. e.:

$$\mathbf{x}^* \in \mathbf{X} \mid f(\mathbf{x}^*) \geq f(\mathbf{x}) \quad \forall \mathbf{x} \in \mathbf{X}, \quad (3.9)$$

if, and only if \mathbf{x}^* is a finite value.

3.2.2 Mathematical Representation

Similar to other evolutionary algorithms, DE starts the searching process with M individuals whose positions are represented by \mathbf{x}_i . Thus, for a \mathbb{R}^2 search space:

$$\mathbf{x}_i = [x_1 \ x_2]_i. \quad (3.10)$$

Assuming K generations for the optimization process, each trial performs *Mutation*, *Recombination* and *Selection*, as described below:

- **Mutation** expands the search space by giving ways for generating new individuals. For all \mathbf{x} individuals in each iteration k , the process chooses four of them \mathbf{x}_i , \mathbf{x}_{r_1} , \mathbf{x}_{r_2} and \mathbf{x}_{r_3} , with $i \neq r_1 \neq r_2 \neq r_3$. The individual \mathbf{x}_i is called *target vector* and the individual \mathbf{x}_{r_1} is added to the weighted difference between \mathbf{x}_{r_2} and \mathbf{x}_{r_3} given by:

$$\mathbf{v}_i = \mathbf{x}_{r_1} + \xi \cdot (\mathbf{x}_{r_2} - \mathbf{x}_{r_3}), \quad (3.11)$$

where ξ is the *mutation factor* and \mathbf{v}_i is the *donor vector* for the k -th iteration.

- **Recombination** incorporates solutions that resulted in successful fitness performance previously. This process generates the *trial vector* \mathbf{u}_i from a combination of target, \mathbf{x}_i , and donor vectors, \mathbf{v}_i . Each vector position is denoted by j . Giving ς as the probability that elements of donor vector replace elements of the target vector – the *crossover rate* – and giving $\varphi[j]$ as a uniform random variable, we have:

$$\mathbf{u}_i[j] = \begin{cases} \mathbf{v}_i[j], & \varphi[j] \leq \varsigma \text{ OR } j = \iota, \\ \mathbf{x}_i[j], & \varphi[j] > \varsigma \text{ AND } j \neq \iota, \end{cases} \quad (3.12)$$

where ι is a discrete random variable $\in [1, 2, \dots, N]$ which avoid \mathbf{u}_i to become equal to \mathbf{x}_i – at least one value of the donor vector \mathbf{v}_i will be propagated to its offspring \mathbf{u}_i .

Figure 3.2 shows how recombination process works: the trial vector will be filled by elements of either the target or donor vectors, if conditions are satisfied (3.12).

- **Selection** compares the fitness values provided by the i -th trial and the target vectors. If the trial vector results in better fitness, the individual that provides the target vector is replaced by the trial vector as shown:

$$\mathbf{x}_i = \begin{cases} \mathbf{u}_i, & \text{if } \eta(\mathbf{u}_i) \leq \eta(\mathbf{x}_i), \\ \mathbf{x}_i, & \text{otherwise.} \end{cases} \quad (3.13)$$

These processes of mutation, recombination and selection are repeated until the

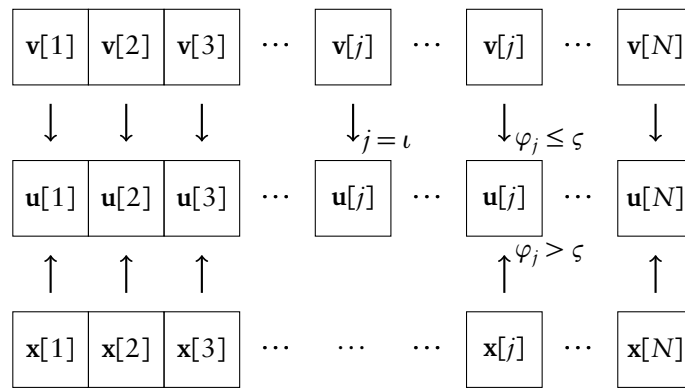


Figure 3.2: Recombination process in DE

optimization criterion is reached or until at most K generations are simulated, as shown in Figure 3.3. Assuming a 2-dimensional search space, the update of individuals by these three processes is graphically shown in Figure 3.4.

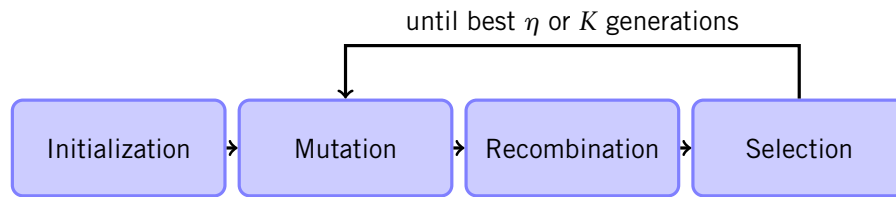


Figure 3.3: DE optimization process flowchart

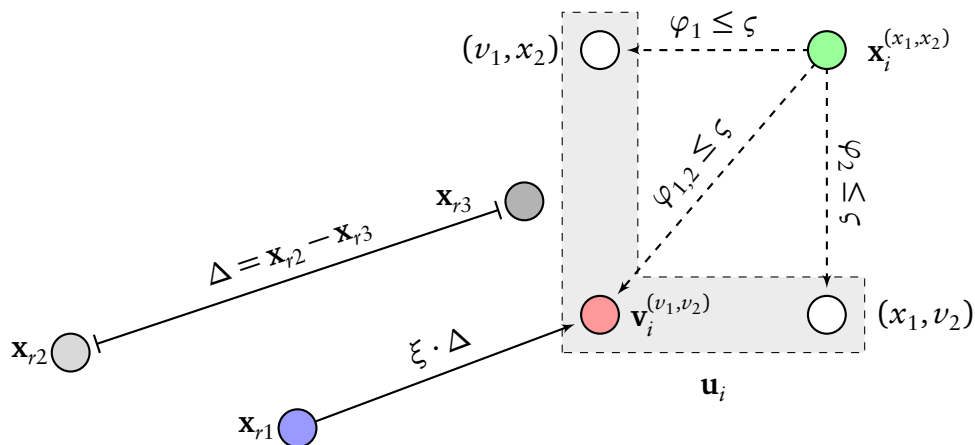


Figure 3.4: Update of individuals in DE

The performance of DE can be improved by adjusting the mutation factor, ξ , crossover rate, ς , and the number of individuals, M .

3.2.3 Simulation Chain

A generic simulation chain for DE is shown in Algorithm 2 by providing the mutation factor, ξ , and crossover rate, ς .

Algorithm 2 DE algorithm

```

1: Define fitness target  $\eta^*$ , mutation factor  $\xi$ , crossover rate  $\varsigma$ 
2: Set up initial target vectors  $\mathbf{x}$ 
3: for all Individuals  $\mathbf{x}_i$  do
4:   Set positions and get their fitness  $\eta_i$ 
5: end for
6: Get best fitness  $\eta_{best}$  of all  $\eta_i$ 
7: while  $\eta_{best} \geq \eta^*$  do
8:   Choose random integers  $i \neq r1 \neq r2 \neq r3$ 
9:   donor vector
10:   $\mathbf{v}_i \leftarrow \mathbf{x}_{r1} + \xi \cdot (\mathbf{x}_{r2} - \mathbf{x}_{r3})$  (3.11)
11:  for all Positions  $j$  do
12:    Compute random integer  $\iota$  and random scalar  $\varphi$ 
13:    Get the trial vector
14:    if  $\varphi \leq \varsigma$  or  $j = \iota$  then
15:       $\mathbf{u}_i[j] \leftarrow \mathbf{v}_i[j]$  (3.12)
16:    end if
17:    if  $\varphi > \varsigma$  and  $j \neq \iota$  then
18:       $\mathbf{u}_i[j] \leftarrow \mathbf{x}_i[j]$  (3.12)
19:    end if
20:  end for
21:  Compute fitness  $\eta(\mathbf{u}_i)$  and  $\eta(\mathbf{x}_i)$ 
22:  if  $\eta(\mathbf{u}_i) \geq \eta(\mathbf{x}_i)$  then
23:     $\mathbf{x}_i \leftarrow \mathbf{u}_i$ 
24:     $\eta_{best} \leftarrow \eta(\mathbf{u}_i)$ 
25:  end if
26: end while

```

3.3 Summary of Optimization Techniques

This chapter briefly discussed the PSO and DE optimization techniques, which are suitable for performing spatial search on multi-modal non-linear fitness spaces. These methodologies, as described in Chapter 1, were already used for network planning in a couple of works, thus, these methods are expected to present good performance when using different fitness approaches. The following Chapter 4 describes characteristics and parameters of modelled regions, environment propagation model, optimization algorithms, performance metrics and fitness functions considered in this thesis.

4. SYSTEM MODEL

CHOOSING a proper system model is relevant to perform a fair comparison of optimization techniques and to simulate how these methods could work using real environment data. There are some techniques to generate a real-based region, which placement of UEs and BSs not only looks like actual deployment from operators, but also presents similar properties, such as coverage probability. This chapter discusses the generation of environments with different BS placement layouts and traffic characteristics.

4.1 Multi-cell Scenario

The *multi-cell scenario* is composed by sets of BSs and UEs distributed over the coverage area and can be generated by many ways, given strategies for placing BSs and modelling UE traffic. This section discusses three methodologies for deploying BSs: *grid layout*, *stochastic geometry* and *based on real data*.

4.1.1 Grid Layout

The grid layout is widely used to represent a cellular network, which is composed by BSs distributed in a hexagonal lattice with fixed distance from each other, as shown in Figure 4.1a. The recommendation in [36] adopts a distance equals 500m between BSs (Inter-site Distance (ISD)) and urban-microcell fading environment for path loss and shadowing.

4.1.2 Stochastic Geometry

Stochastic Geometry (SG) can represent the randomness of an actual wireless network allowing to study the average behaviour over many spatial realizations of a network whose nodes are placed according to some probability distributions [37]. This network randomness is particularly verified when working with Heterogeneous Networks (HetNets). In this scenario, due to the increasing number of nodes, network elements are placed to satisfy ad-hoc requirements.

There are many point processes used to generate regions such as the Poisson Point Process (PPP) and the Hardcore Point Process (HCPP). The PPP is used to represent up to infinity UE nodes within a finite service area [38] while HCPP is suitable for placing

BSs because it requires a minimum distance R for deploying nearby bases. Indeed, the BS locations appear to form a more regular point pattern than the PPP because of repulsion between points [39].

A PPP is composed by a set Π of points from which any subset $B \subset \Pi$ is composed by Poisson random variables, as follows:

$$\Pi = \{x_i, i = 1, 2, 3, \dots\} \subset \mathbb{R}^d \text{ if, and only if } B \subset \Pi \text{ is a Poisson variable,} \quad (4.1)$$

where \mathbb{R}^d is the d -dimensional search space.

An HCPP is a repulsive point process where no two points of the process coexist with a separating distance not smaller than a predefined hard core parameter R :

$$\Pi = \{x_i, i = 1, 2, 3, \dots\} \subset \mathbb{R}^d \text{ if, and only if } \|x_i - x_j\| \geq R; \forall x_i, x_j \in \Pi. \quad (4.2)$$

The definition of regions with PPP and HCPP points require definition of density λ for UEs and BSs, usually given in number of points per area unity. Figure 4.1b shows the BSs deployment deploying according to a HCPP process with $R = 70\text{m}$.

4.1.3 Based on Real Data

The real scenario is based on real information of BS positions found in some databases such as Brazilian Telecommunications Regulatory Agency (ANATEL) database [40], which gives data from operators in Global Positioning System (GPS) coordinates. Figure 4.1c shows an example of BSs existing in a Brazilian city.

The evaluation of fading properties requires conversion of distance dependent parameters originally given in GPS coordinates to meters in order to evaluate the distances between points, such as *Haversine* (great circle) method [41]. Given two points with latitude φ_1, φ_2 and longitude λ_1, λ_2 , let $\Delta\varphi = \varphi_2 - \varphi_1$ and $\Delta\lambda = \lambda_2 - \lambda_1$:

$$a = \sin^2\left(\frac{\Delta\varphi}{2}\right) + \cos(\varphi_1) \cdot \cos(\varphi_2) \cdot \sin^2\left(\frac{\Delta\lambda}{2}\right),$$

$$c = 2 \cdot \text{asin}(\sqrt{a}).$$

Thus, the distance between these two points d is given by:

$$d = R_{\text{earth}} \cdot c, \quad (4.3)$$

where $R_{\text{earth}} = 6,371 \text{ km}$, assuming a spherical surface of earth.

All scenarios described in subsections 4.1.1, 4.1.2 and 4.1.3 are shown in Figure 4.1, which Grid and SG BS layouts are described in meters while actual data is represented in GPS coordinates.

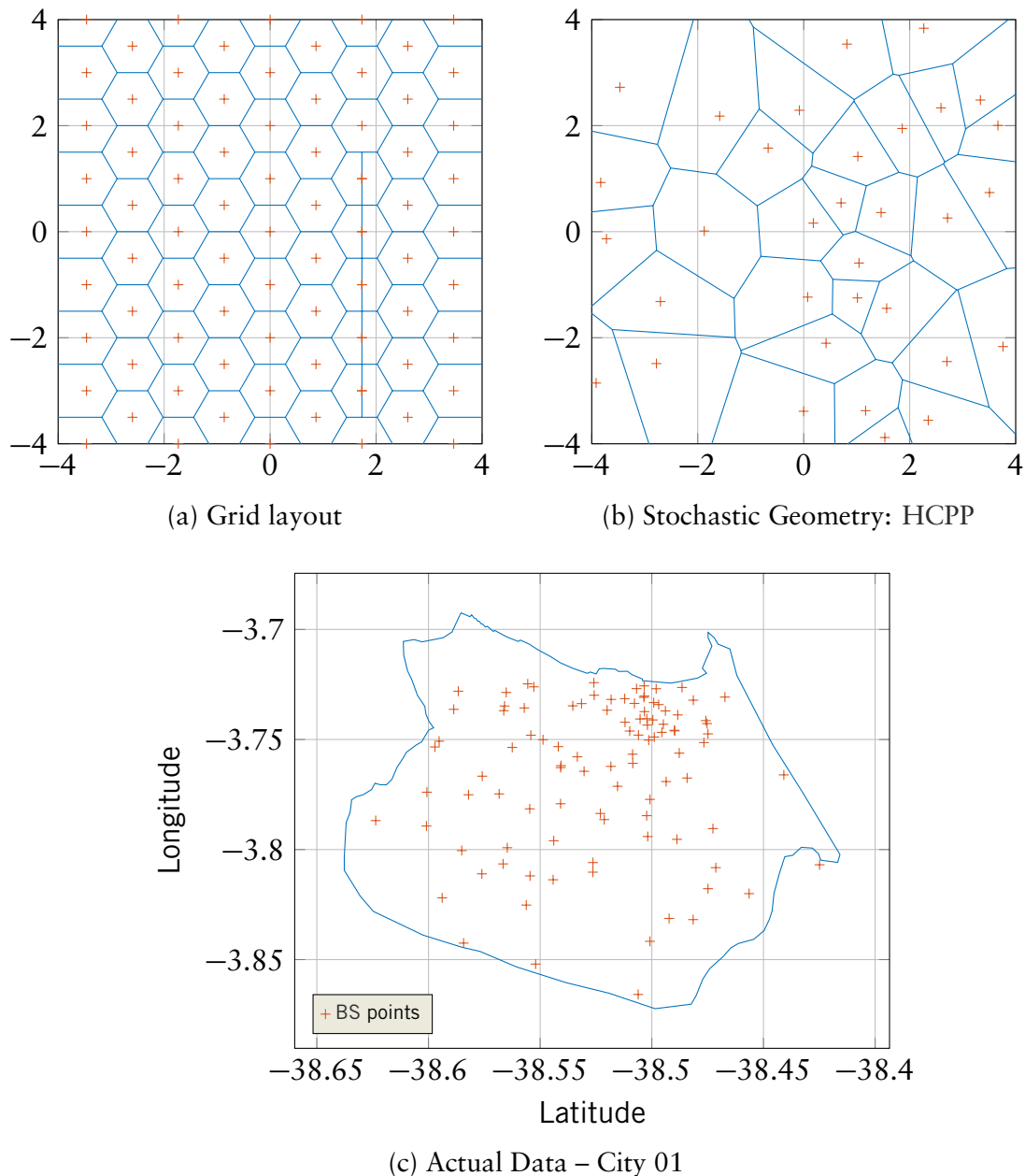


Figure 4.1: Layouts for BS initial deployment regions

4.2 UE Traffic Positioning and Representation

The characterization of demanded traffic can be done by the geographical and demographical aspects of the service area [42]. The UEs placement can be implemented by many ways in order to capture specific characteristics in the simulation, especially the

heterogeneity of traffic demand in specific locations of network. In other words, the UEs deployment represents the traffic inside the region of interest. In order to perform this modelling, for the following methods supposing a set of m UEs with positions $UE_m(\mathbf{x})$, \mathbf{x} is the spatial location of UE and the traffic associated to UE_m will be denoted by γ_m .

For a set of N BSs, assuming the throughput demanded by each BS, n , as $C_{m,n}$, and supposing M^* users connected to that base, the total required throughput can be interpreted as:

$$C_{m,n} = \sum_{m=1}^{M^*} C_m. \quad (4.4)$$

Thus, for user required throughput γ_m :

$$C_{m,n} = \sum_{m=1}^{M^*} \gamma_m. \quad (4.5)$$

4.2.1 Randomly Heterogeneous UEs Deployment

In this technique, all user points are assumed as demanding traffic of the same kind. Thus, high traffic regions can be interpreted as those where a larger amount of UE points can be found. Using this methodology, the evaluation of outage or satisfaction analysis is done by assessing single UEs performance.

The placement of users non-uniformly distributed is defined by setting up regions whose probability of UE be inserted inside differs from each other. The set of $UE_m(\mathbf{x})$ has a probability to be inserted depending on \mathbf{x} position.

Since the users' required throughputs are equal to all points, i.e., $\gamma_m = \gamma^*$, (4.5) can be rewritten as:

$$\begin{aligned} C_{m,n} &= \sum_{m=1}^{M^*} \gamma^*, \\ C_{m,n} &= M^* \cdot \gamma^*, \end{aligned} \quad (4.6)$$

which is basically the number of connected UEs scaled to the throughput γ^* . The generation of this kind of environment assumes multiple subregions with varying density of users. Assuming the global environment as R , a region R_k contains particular aspects in terms of traffic demand or user density such that $R_k \subset R$. The region R_k contains n_k users, so the density of users λ_k can be denoted by:

$$\lambda_k = \frac{\text{area}(R_k)}{n_k}, \quad (4.7)$$

interpreted as number of UEs per unity of area.

The simulation of two UE configurations for City 1 depends on this method. The first configuration considers that the user density varies according to each neighbourhood, called *peak traffic*, t_{peak} . This deployment bases on gathering population and area of City 1 neighbourhoods available in [43], which are used to generate a λ_k for each neighbourhood. The users were placed using PPP method inside every subregion, and varying the λ parameter as shown in Figure 4.2. In the second configuration, a uniform deployment of users is performed inside City 1 boundaries using a PPP with the same λ parameter for all regions, which is called *average traffic*, t_{avg} . Figures 4.3a and 4.3b show peak and average traffic configurations, respectively.

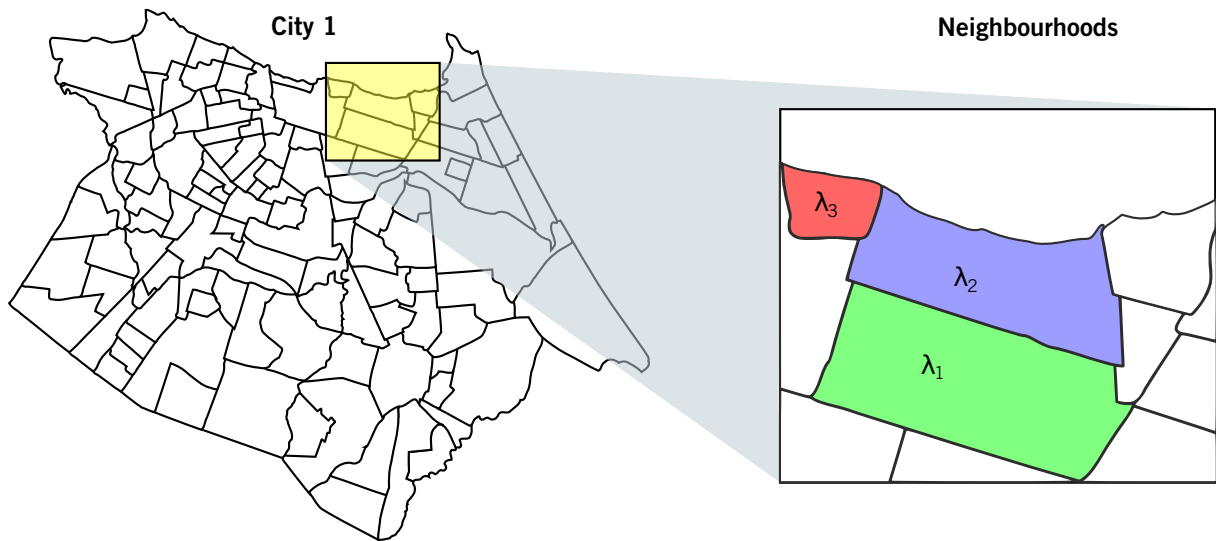


Figure 4.2: Variation of population density λ according to each neighbourhood

4.2.2 Grid UEs Deployment With Traffic Density

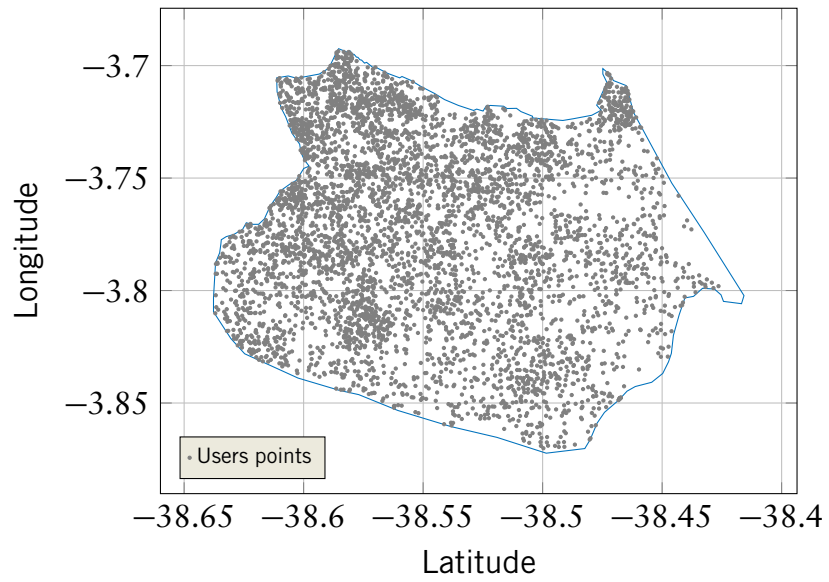
This method sets a grid containing a fixed quantity of UEs with different traffic demands. The estimation of traffic metrics per BS is done by using (4.5), which provide total required throughput given traffic per user γ_m .

Supposing the region $R_k \subset R$, the density of users λ_k for this method is denoted by:

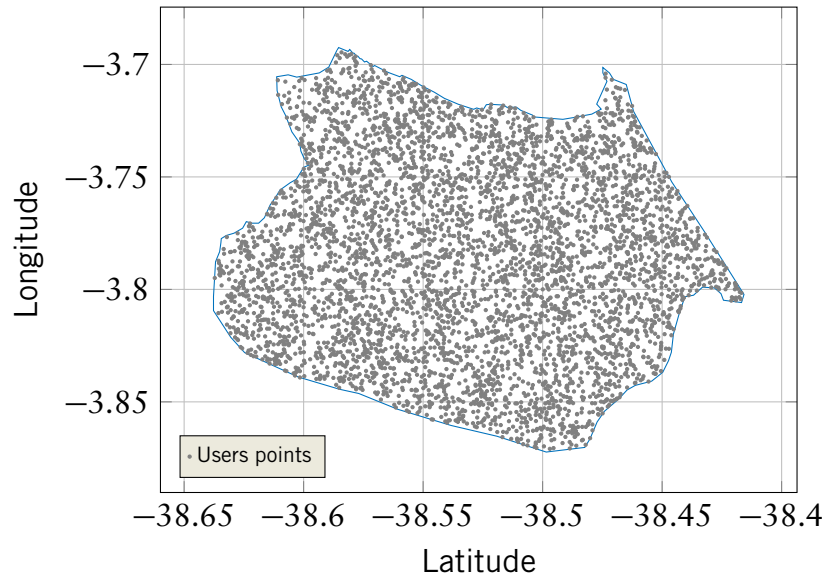
$$\lambda_k = \frac{\text{area}(R_k)}{n_k} = \lambda^*, \quad (4.8)$$

for any region R_k which results in a fixed density λ^* in comparison with (4.7). This technique is used to set up users' traffic for Grid and SG scenarios.

Considering the UEs deployment described in Sections 4.2.1 and 4.2.2, Figure 4.4 shows an example of UEs deployment into a map divided into three regions considering



(a) Peak traffic



(b) Average traffic

Figure 4.3: Traffic demand estimation and BS positions for City 1

different values of density λ in Figure 4.4a and demanded traffic of users γ in Figure 4.4b.

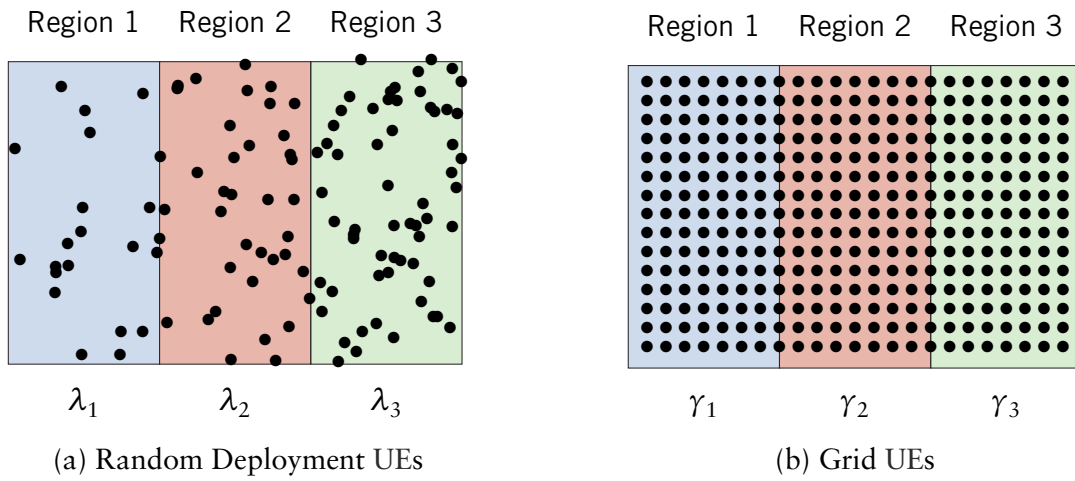


Figure 4.4: Diagram of UEs deployment

4.3 Simulation Cases

Assuming all described scenarios previously in Sections 4.1 and 4.2, the following simulation test cases are defined:

- **Case 1: Grid deployment for BSs and UEs; fixed distribution of UEs:** This arrangement configures BSs in a grid layout by defining their radius and places UEs in grid distribution with homogeneous traffic demand, i.e., $\gamma = \text{constant}$ for any UE. The network is initially designed with N BSs, from which it is removed 1 or 2 BSs. The optimization process tests PSO and DE, by placing one or two bases in the modified grid and exhibits results for fitness evolution and distribution of optimized points.
- **Case 2: Stochastic Geometry deployment for BSs and UEs, homogeneous distribution for UEs:** This configuration assumes BSs deployed under a HCPP process and UEs as PPP process. Each distribution of BSs and UEs presents its own density λ . This model tests the placement of multiple BSs: 1, 2 and 4 using PSO and DE, exhibiting fitness performance only.
- **Case 3: Actual Data for BSs and traffic estimation of UEs:** The third case considers the region of City 1 with actual deployment of BSs and two density of users: the first corresponds to the heterogeneous population data of a city and the second is a random deployment of users using PPP with fixed density. Only PSO is used in this case, which tests the placement of 4, 8, 16 and 32 new bases.

4.4 Fitness Functions

Using functions described in Section 2.3, two objective functions φ_1 and φ_2 are defined below, considering the selection of $\alpha = 4$ in (4.9a) to adjust the shape φ_1 in order to penalize points which result in high overload for new bases as well as regions where new bases would present low demand.

$$\varphi = \begin{cases} \varphi_1 = \eta_1; & \alpha = 4, \\ \varphi_2 = \eta_2. \end{cases} \quad (4.9a)$$

$$(4.9b)$$

As described in Section 2.3, the fitness function φ_1 attempts to place new bases where they would serve traffic demand very close to their throughput limit and the function φ_2 combines maximization of capacity sensed by users with load balancing of BSs' demand.

The use of each objective function in all cases is described below:

- **Cases 1 and 2** are evaluated with φ_1 (4.9a) and φ_2 (4.9b);
- **Case 3** is verified with function φ_2 when combining influences of average and peak traffic shown in Section 4.2. Given the function $\eta_2 = J \cdot \overline{C}$ (2.21), the contribution of peak and average traffics for η_2^{peak} and η_2^{avg} will be denoted by:

$$\eta_2^{peak} = J_{peak} \cdot \overline{C_{peak}}, \quad (4.10)$$

$$\eta_2^{avg} = J_{avg} \cdot \overline{C_{avg}}. \quad (4.11)$$

Thus, these both influences were considered to generate the objective function φ_2^* (4.12):

$$\varphi_2^* = \eta_2^{peak} + \eta_2^{avg}. \quad (4.12)$$

4.5 Environment Parameters

After creating configurations for UEs and BS placement, the environment parameters are defined for obtaining essentially received power for each UE by all bases, which are described by 3rd Generation Partnership Project (3GPP) recommendation in [36]; the *urban-micro* environment is used for simulation cases 1 and 2 while case 3 is performed on the *urban-macro* environment. Main parameters are shown in Table 4.1 and Table 4.2.

Table 4.1: Large-scale fading model parameters for urban-micro environment

Parameter	Value	Unit
Inter-site distance (Case 1 only)	500	m
Frequency	2	GHz
Noise Power	-124	dBm
Minimum distance UE to BS	20	m
BS transmit power	38	dBm
UE transmit power	24	dBm
Path loss model for cellular links	$34.5 + 38\log_{10}(d)$	dB, d in m
Lognormal shadowing standard deviation	10	dB

Table 4.2: Large-scale fading model parameters for urban-macro environment

Parameter	Value	Unit
Frequency	2	GHz
Noise Power	-124	dBm
Minimum distance UE to BS	35	m
BS transmit power	46	dBm
UE transmit power	24	dBm
Path loss model for cellular links	$32.2 + 35\log_{10}(d)$	dB, d in m
Lognormal shadowing standard deviation	8	dB

4.5.1 LTE Parameters

Within a BS coverage area, all subscribers connected to the BS will experience different data rates due to the distance-dependent channel effects. The throughput performance for UEs depends also on antenna technology and channel bandwidth. Thus, a realistic configuration must be chosen by defining the following aspects: *data sub-carriers* N_{SC} , *slots per second* N_{SLOTS} , *symbols per second* N_{SYMBOL} , *bits per symbol* β , *code rate* v and *spatial streams* $N_{STREAMS}$, which relates to antenna diversity. These aspects are used to estimate the throughput, τ , for LTE transmissions [44] as follows:

$$\tau = N_{SC} \times N_{SLOTS} \times N_{SYMBOLS} \times \beta \times v \times N_{STREAMS} \quad (4.13)$$

Considering τ as the throughput limit, and recovering definition of the maximum throughput ℓ in (2.3.1), one has:

$$\ell = \tau. \quad (4.14)$$

The definition of the maximum acceptable throughput of BSs requires specifications of all these parameters. The objective is determine how much traffic can be demanded to a single base. Assuming LTE common parameters, Table 4.3 specifies inputs for (4.13) for simulation cases 1 and 2. Macro cells adopting Multiple-Input Multiple-Output (MIMO)

Table 4.3: Parameters for LTE throughput (Simulation Cases 1 and 2)

Parameter	Value	OBS.
BW	20 MHz	
N_{SC}	1200	20 MHz bandwidth
N_{SLOTS}	2000	
$N_{SYMBOLS}$	7	
β	6	64-QAM
ν	$\frac{4}{5}$	
$N_{STREAMS}$	4	MIMO 2×2
Parameter	Value	Unit
τ	322.56	Mbps
τ/BW	16.128	bps/Hz

2×2 result in a maximum throughput per BS equals 322.56 Mbps or 16.128 bps/Hz, considering a 20 MHz bandwidth.

The simulation case 3 does not suppose maximum throughput per base, resulting in the use of fitness function φ_2^* only. The changes on Table 4.3 parameters for this simulation case consider a bandwidth of 10 MHz and $N_{STREAMS} = 1$ in a Single-Input Single-Output (SISO) system, instead of adopting original values for simulation cases 1 and 2.

4.5.2 Traffic Model

The traffic model defines characteristics of network usage or demands from users, which is set after generating UEs positions in regions of each case. The *full buffer* model, which assumes all UEs present continuous transmission in UL and DL is known to be impracticable because in realistic settings, users are not continuously transmitting [45]. Despite this aspect, this model has been extensively used in many works that aim to measure spectral efficiency of systems.

4.6 Optimization Techniques Parameters

Each optimization techniques described in Chapter 3 requires the definition of many parameters, which affect the performance by adjusting exploration and exploitation stages. The following subsections exhibit main parameters for PSO and DE.

Table 4.4: Parameters for PSO optimization – Simulation Cases 1 and 2

Cases 1 and 2 – Grid and Stochastic Geometry								
No. of PSO repetitions	No. of iterations	No. of Individuals	Inertia Attributes		Social Influence	Persistence		No. of BSs
N_{trials}	K	M	w_0	w_K	c_{gB}	c_{pB}	N_{BS}	*Grid Only
50	100	[16, 32]	1	0.4	2	1		[1*, 2*, 4]

Table 4.5: Parameters for PSO optimization – Simulation Case 3

Simulation Case 3 – Actual Data									
No. of PSO repetitions	No. of iterations	No. of Individuals	Inertia Attributes		Social Influence		Persistence		No. of BSs
N_{trials}	K	M	w_0	w_K	$c_{gB}[0]$	$c_{gB}[K]$	$c_{pB}[0]$	$c_{pB}[K]$	N_{BS}
50	100	[16, 32]	1	0.4	2	0.5	1	2	[8, 16, 32]

4.6.1 PSO Parameters

Table 4.4 exhibits simulation parameters for Cases 1 and 2 and Table 4.5 shows parameters for case 3, described in Section 4.3. Cases 1 and 2 assumed variation in inertia weights and fixed social influence and persistence attributes. In case 3, PSO performs optimization with variation on social influence and persistence as described in 3.1.3. The number of new BSs for placing varies from {1,2} in Case 1, {1,2,4} in Case 2 and {8,16,32} in Case 3.

4.6.2 DE Parameters

Table 4.6 shows simulation parameters for Cases 1 and 2 described in Section 4.3. Mutation factor and crossover rate are fixed for both cases. The optimization attempts to deploy 1 or 2 new BSs in described scenarios. The number of iterations and repetitions is equal to PSO case in order to compare performance.

Table 4.6: Parameters for DE optimization – Simulation Cases 1 and 2

Cases 1 and 2 – Grid and Stochastic Geometry				
No. of DE repetitions	No. of iterations	Mutation Factor	Crossover Rate	No. of BSs
N_{trials}	K	ξ	ς	M (*Grid Only)
50	100	1	0.4	[1*, 2*, 4]

4.7 Network Performance Metrics

The fitness functions described in Section 4.4 are appropriate to lead optimization process towards values which result in good fitness, but the impact on performance of network also needs evaluation.

There are some common metrics which are used to measure network performance and QoS, from which the *Capacity* and *Outage* of users are related to how users sense network performance. The system capacity was previously described in Section 2.1, which defines total capacity as the sum of sensed capacities of users.

In fading channel environments users experience rapidly changes on signal strength and, usually, there is a minimum received power level P_{min} which is impossible to perform communication if signal drops below this set-point. Considering the shadowing, which is log-normally distributed, there is a probability of received signal P_r falling below P_{min} : the *outage probability* (p), which depends on the combination of path-loss PL and shadowing standard deviation σ_χ as follows [22]:

$$p(P_r \leq P_{min}) = 1 - Q\left(\frac{P_{min} - PL}{\sigma_\chi}\right), \quad (4.15)$$

where $Q(z)$ is defined as the probability that a Gaussian random variable x with mean zero and variance one is bigger than z .

These two metrics are evaluated in simulation case 2, the stochastic geometry-based, using the simulation parameters described in previous sections and urban-micro environment shown in Table 4.1. The estimation of outage considers the UE received power from its connecting BS, whose the minimum received power is defined as $P_{min} = -100\text{dBm}$.

4.8 Summary of System Model

This chapter presented methodologies for generating the multi-cell scenario and setting up users' traffic and parameters for the environment and optimization methods. The performance comparison between PSO and DE techniques will be described in Chapter 5.

5. RESULTS

THIS chapter discusses results for each of the simulation cases described in Section 4.3 in terms of fitness performance, optimized points and impact on network efficiency using PSO and DE. Here, advances using the three simulation cases described earlier in Section 4.3 will be shown.

5.1 Case 1 – Grid layout

The Grid layout simulation case – Case 1 – was described in Section 4.3, which consists in a grid region with hexagonal layout for bases. For performing simulations, it was created a region with sets of BSs and UEs presenting the same traffic for all points. The major parameters for regions in Case 1, such as the region area and number of UEs, are shown in Table 5.1.

5.1.1 Fitness Function

Figures 5.1a and 5.1b exhibit the fitness functions φ_1 and φ_2 , respectively, described in Section 4.4, for a grid region considering the following situations:

- **Case A:** removing the BS located at (0, 0);
- **Case B:** removing bases at (0, 0) and (0, 0.5).

The elimination of these bases affects fitness functions because network demands of UEs previously covered by removed the BSs increase as much as their sensed capacities lows: users will no longer be served by these bases. Supposing these facts, there is expectation of high fitness values in these locations, which is confirmed in Figure 5.1, where the higher the fitness function values become, the closer the positions approaches the removed points. It is good to remind that fitness functions are evaluated for inserting

Table 5.1: Parameters for Simulation Case 1 – Grid Layout

Simulation Case 1				
Region area (A)	No. of BSs	No. of Removed BSs	No. of UEs	Traffic density per area (γ/A)
$4km^2$	17	1 (case A), 2 (case B)	4096	$380Mbps/km^2$

a single new base, thus, it is hard to graphically present the impact of placing two bases in the environment. Furthermore, it would be required to evaluate fitness for all combination of two sets N points, thus, testing N^2 points for evaluating fitness performance.

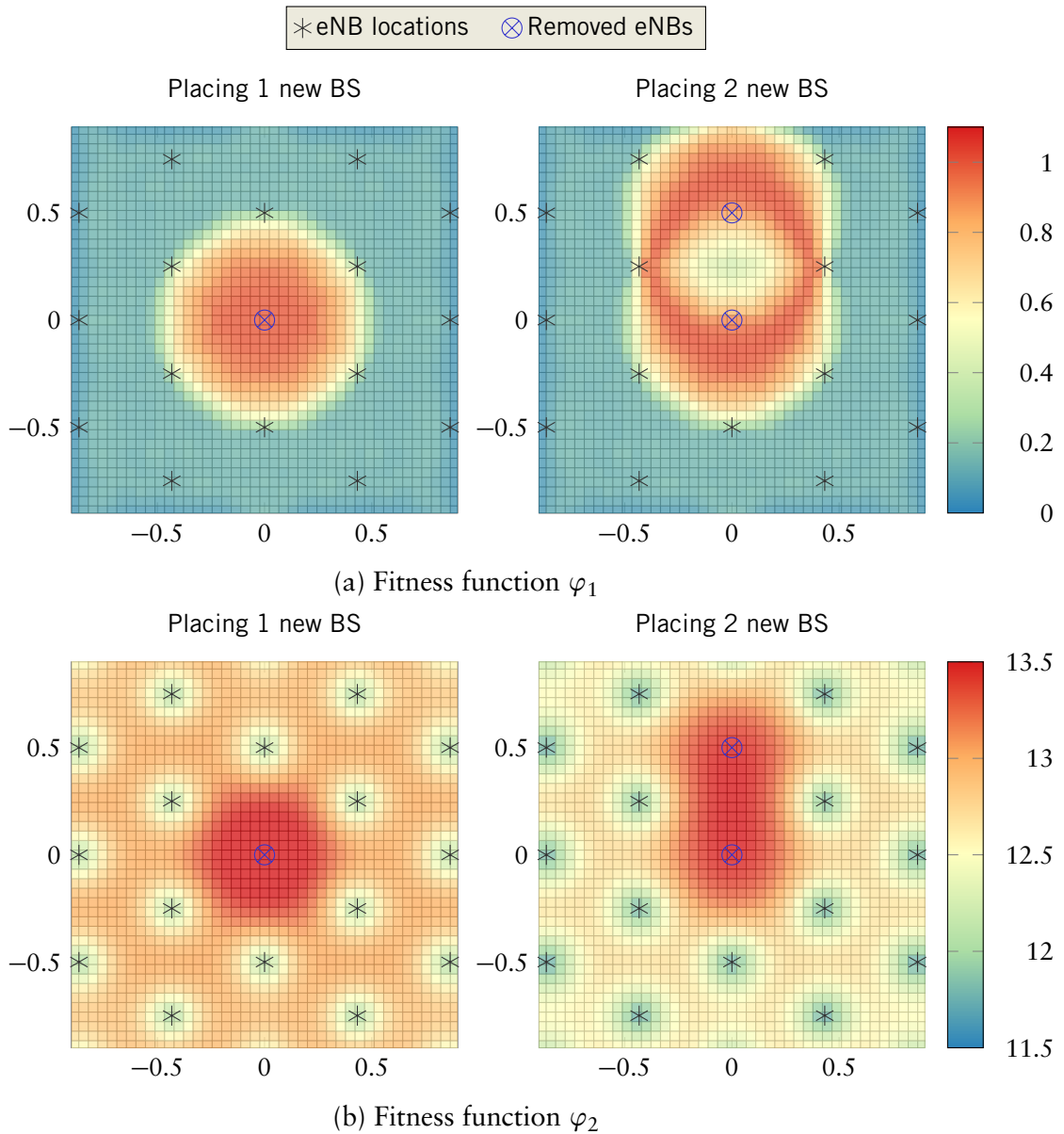


Figure 5.1: Fitness functions φ in Grid layout

For placing a single BS, it is expected for optimization algorithms to find solutions at locations with the highest fitness values, but it could probably be different when inserting multiple bases simultaneously because the position \mathbf{x} of eNB_1 will affect fitness performance of remaining bases.

5.1.2 Performance Results

The results show the improvement on the values of the fitness functions for both PSO and DE methods. PSO shows advantages and better solutions when using a lower quantity of individuals than DE, such as in the 8 individuals case shown in Figure 5.3. The mean final fitness values found by PSO, for fitness functions φ_1 and φ_2 , respectively, are 1.00 and 13.45, as shown in Table 5.2, when using 8, 16 or 32 individuals. For all variations on the number of individuals, the mean optimized point after 50 trials is also described in Table 5.2.

Table 5.2: Fitness results and best points found by PSO in 50 trials

Fitness function	No. of Individuals	Fitness ($K = 100$)	Best Points (Mean)	Std. deviation (Best Points)
φ_1	8	1.000	(0.005, -0.006)	0.039
	16	1.000	(0.000, 0.007)	0.038
	32	1.000	(0.007, 0.000)	0.037
φ_2	8	13.449	(0.001, 0.000)	0.004
	16	13.449	(0.000, 0.000)	0.004
	32	13.449	(0.000, 0.000)	0.004

Although DE presented a worse performance when using less individuals than PSO, this technique is able to find suboptimal solutions very soon in terms of iterations, as shown in Table 5.3, which the mean number of reached iterations is less than half of total iterations in PSO for 5 of 6 simulation setups – in other words, DE converges in half of the total number of iterations in 50% of trials. The increasing on the number of individuals affects this mean of reached iterations because the less the number of individuals, the less the needed amount of iterations to converge, which CDFs are shown in Figure 5.2.

Table 5.3: Mean number of iterations until DE find best solution

Fitness function	No. of Individuals	Mean Number of Iterations
φ_1	8	26.6
	16	37.1
	32	49.5
φ_2	8	27.7
	16	42.2
	32	56.9

The performance of DE is worse than that of PSO for 8 individuals and all fitness functions at the end of the iterations, but it presents advances as the number of individuals

increases for fitness functions φ_1 and φ_2 as exhibited in Figure 5.3. DE is not able to overtake PSO's performance considering fitness function φ_1 , but it achieves higher fitness at the end of iterations for function φ_2 compared to the PSO case. On the other hand, the standard deviation of mean solution points is lower in PSO in all cases, which means the solutions are more concentrated in the search space than DE's findings.

Table 5.4: Fitness results and best points found by DE in 50 trials

Fitness function	No. of Individuals	Fitness ($K = 100$)	Best Points (Mean)	Std. deviation (Best points)
φ_1	8	0.963	(-0.001, 0.005)	0.130
	16	0.989	(-0.007, -0.006)	0.079
	32	0.999	(0.002, 0.016)	0.050
φ_2	8	13.442	(-0.009, 0.003)	0.187
	16	13.556	(0.012, -0.015)	0.085
	32	13.590	(-0.002, -0.002)	0.044

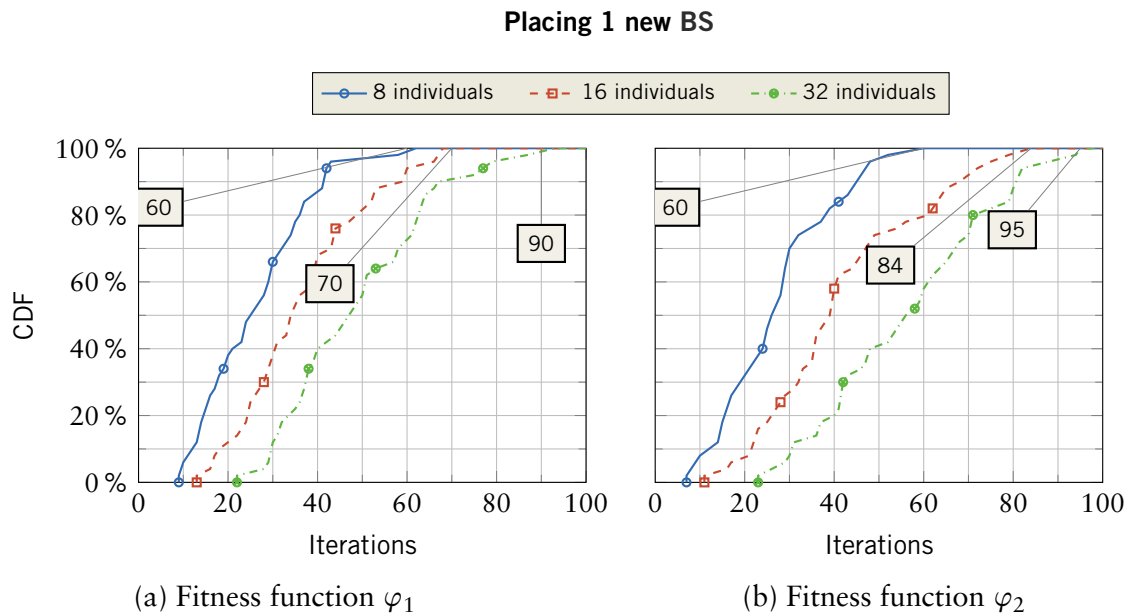


Figure 5.2: CDFs of number of iterations until find best solution in DE – Grid layout

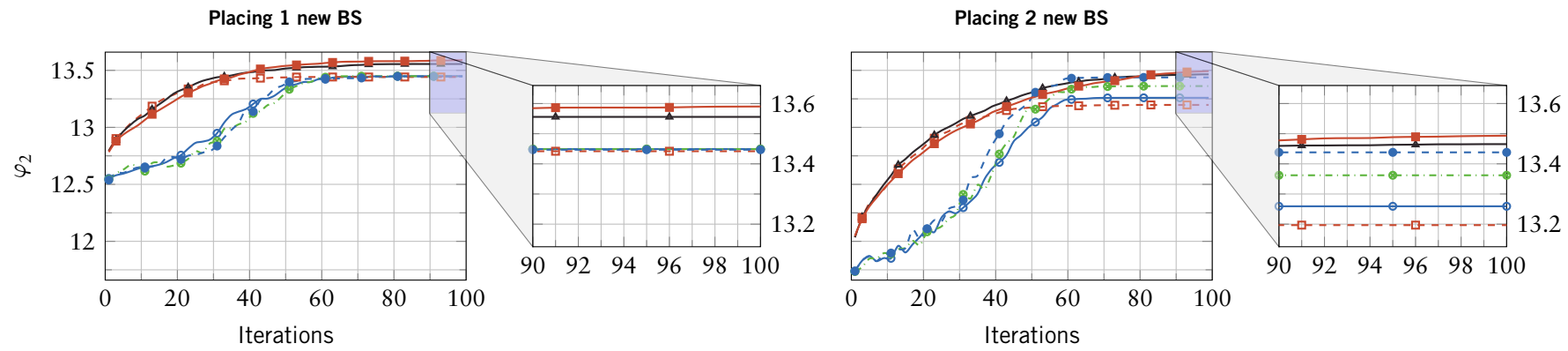
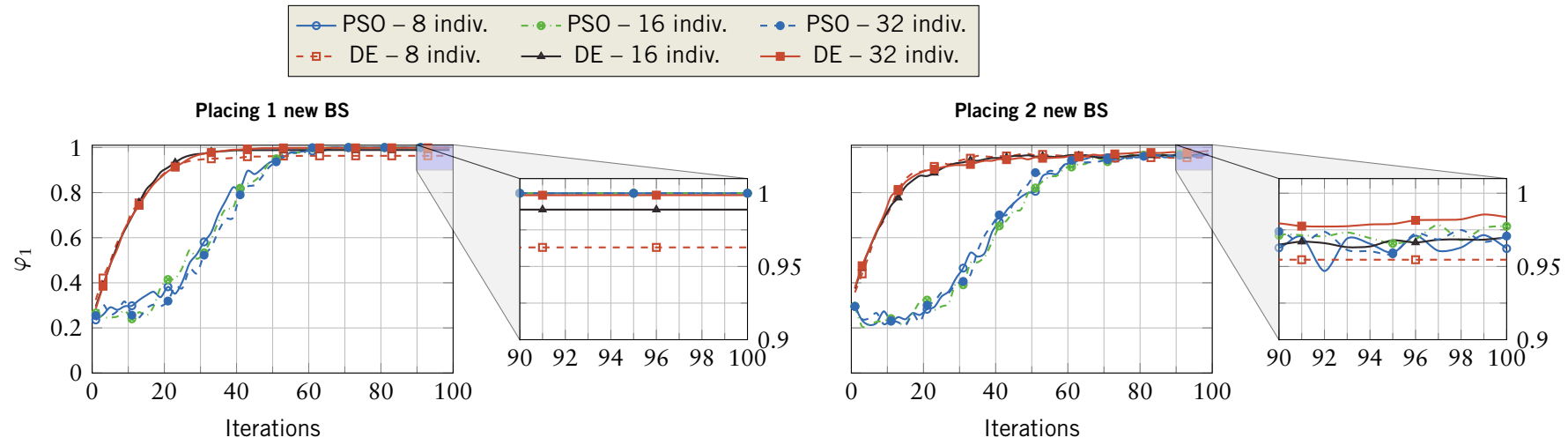


Figure 5.3: PSO and DE performance for 8, 16 and 32 individuals – Grid layout

5.1.3 Optimized Points

The PSO set of optimized points for all fitness functions scenarios, considering cases A and B, showed in Figure 5.4 for 32 individuals. In case A, PSO is able to find solutions very close to the position of the removed BS; indeed, the fitness improves the quality of solutions as shown earlier in Figure 5.3. A group of solutions can be found very close to the excluded points for all fitness function $\{\varphi_1, \varphi_2\}$ as shown previously in Table 5.2.

Due to the contributions of an optimized point from particle P_1 to fitness performance of particle P_2 , the exclusion of two BSs results on a wider distribution of solutions for fitness function φ_1 than the case of placing a single new base. On the other hand, the fitness function φ_2 results in narrowly spread solutions with very low error.

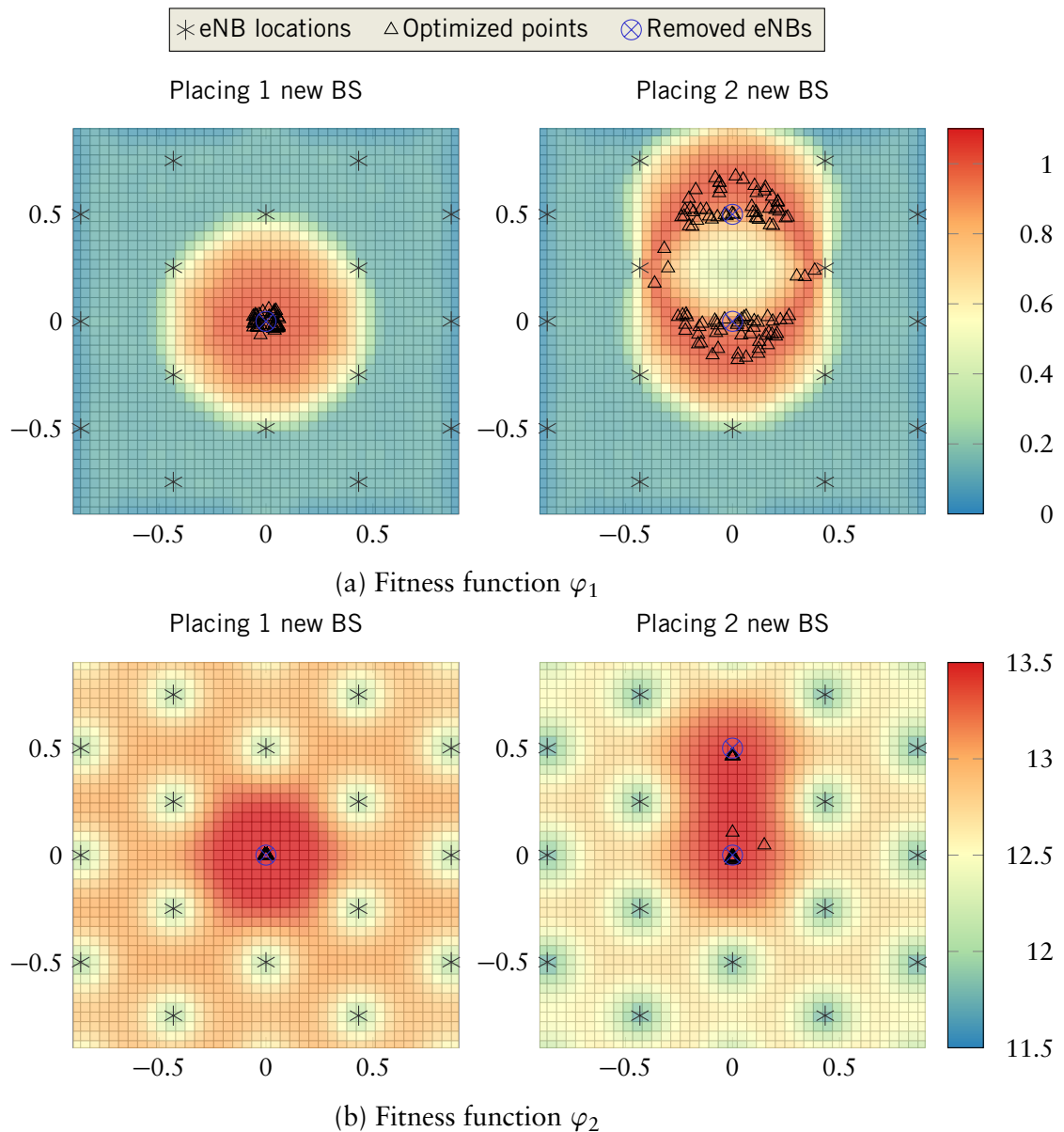


Figure 5.4: PSO performance – Fitness functions φ in Grid layout

The optimized points found by DE are shown in Figure 5.5, analogous to PSO case when placing one or two BSs. DE presents higher standard deviation of mean optimized points than PSO as shown Table 5.4, resulting in a disperse set of solutions as exhibited in Figure 5.5.

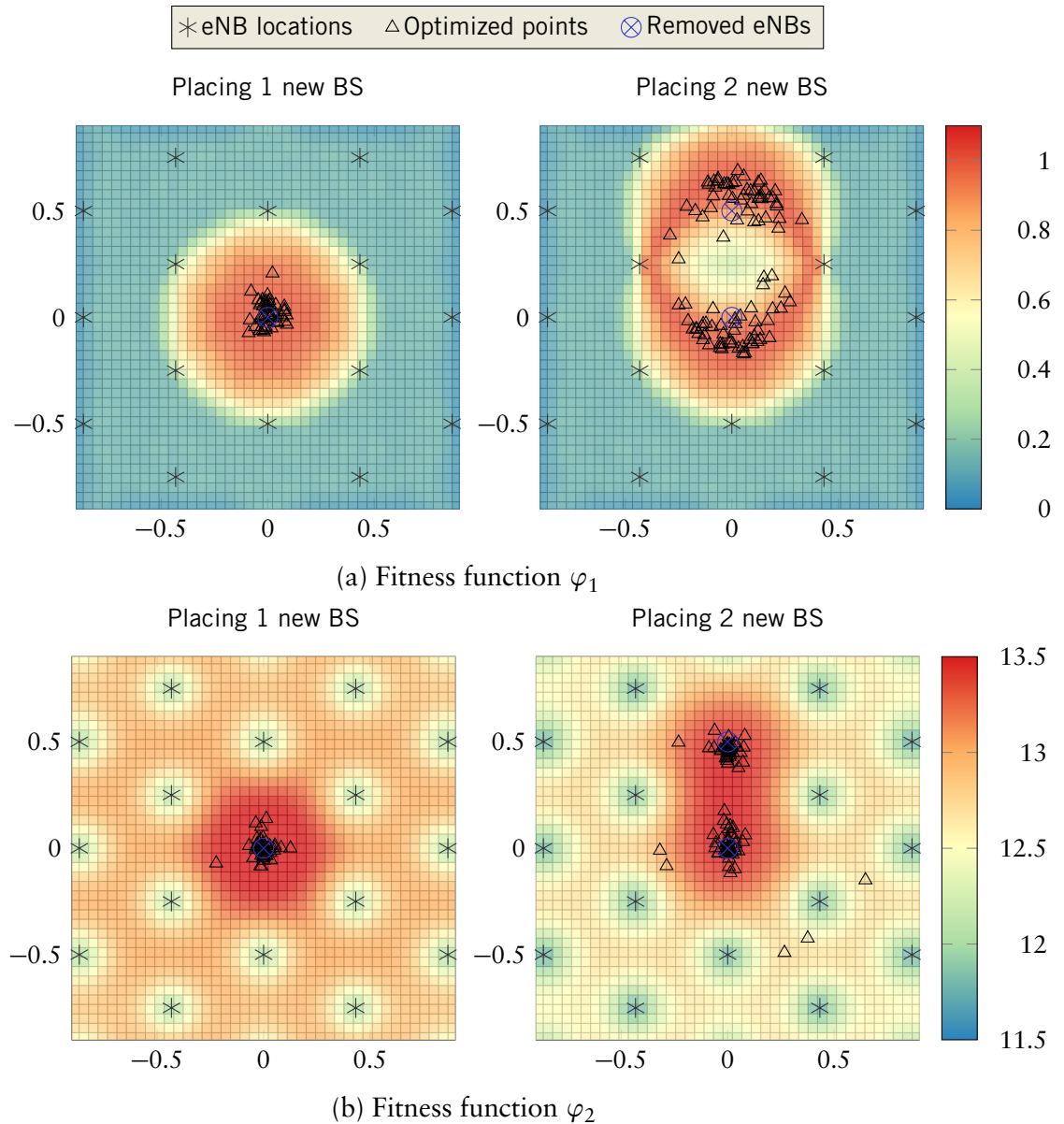


Figure 5.5: DE performance – Fitness functions φ in Grid layout

5.1.4 Summary of Optimization in Case 1

Both PSO and DE are effective to provide sets of results close to removed BS points assuming fitness functions φ_1 and φ_2 . The PSO presents a set of solutions which results in lower standard deviation than DE for all combination of amount of individuals and fitness functions but DE is capable to find good solutions in less than half the number of the PSO iterations in at least 50% of trials.

5.2 Case 2 – Stochastic Geometry

The Stochastic Geometry layout simulation case – Case 2 – was described in Section 4.3. Analogous to Case 1, the region contains sets of BSs and UEs with the same traffic for all points. The major parameters for regions in Case 2 are shown in Table 5.5.

Table 5.5: Parameters for Simulation Case 2 – SG layout

Simulation Case 2			
Region area (A)	Density of BSs (HCPP)	Density of UEs (PPP)	Traffic density per area (γ/A)
$4km^2$	$\lambda_{BS} = 4$	$\lambda_{UE} = 150$	$380Mbps/km^2$

5.2.1 Performance Results

The CDFs shown in Figure 5.6 indicate that more than 50% of trials reached the maximum number of iterations, suggesting that DE has not converged yet at that point, when using function φ_1 . The use of fitness function φ_2 decreases the number of trials which reached K iterations to only 10%. Recovering the results of convergence in Figure 5.2 for the Grid Layout, the convergence decreases as the number of individuals grows.

For the case of placing 2 new bases, which CDFs are shown in Figure 5.7, more than 70% of the individuals in DE trials also reach K iterations for fitness φ_1 . The results of testing fitness functions φ_1 and φ_2 for placing 1 and 2 new bases using DE indicate that the optimization must run as a greedy algorithm, thus, without limit on number of iterations, to perform a proper optimization.

The performance of placing 1, 2 and 4 new BSs with 8, 16 and 32 individuals for PSO and DE in stochastic geometry layout is shown in Figures 5.8, 5.9 and 5.10. PSO presents better mean performance only when using fitness function φ_2 in most cases while DE showed better improvements when using fitness function φ_1 in all comparisons between number of individuals and number of new bases. PSOs has worse performance than DE when using a lower number of individuals for performing searches. The results on fitness function φ_2 show that a large number of individuals benefits PSOs performance and requires DE to run more iterations to converge.

The performance results of fitness functions for the stochastic geometry-based layout are shown in Figures 5.8, 5.9 and 5.10 for 8, 16 and 32 individuals, respectively. When using only 8 individuals for optimization, PSO presents its poorest fitness perfor-

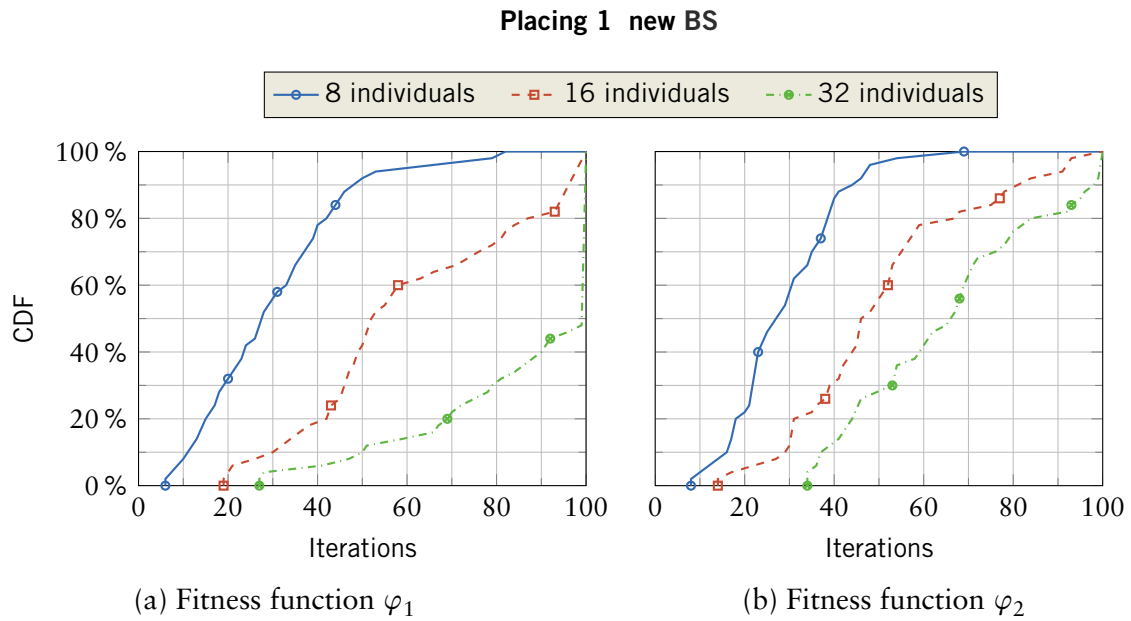


Figure 5.6: CDFs of number of iterations until find best solution in DE when number of new BS = 1 – Stochastic Geometry layout

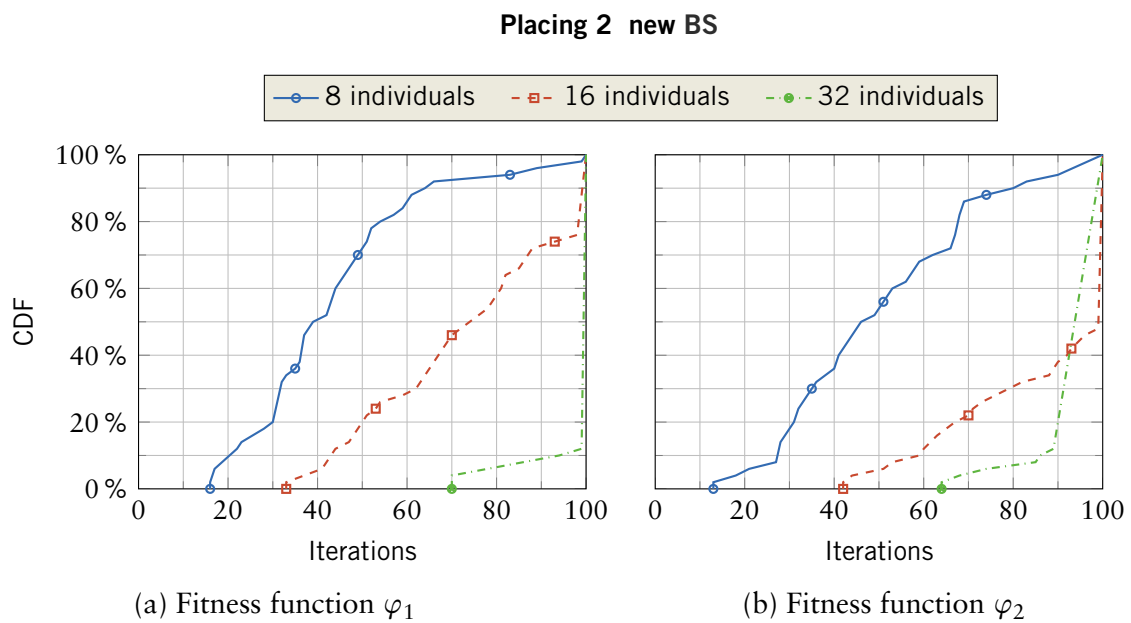


Figure 5.7: CDFs of number of iterations until find best solution in DE when number of new BS = 2 – Stochastic Geometry layout

mance when placing 4 new BSs with fitness φ_1 while DE exhibited its poorest results when placing 1 single BS with fitness φ_2 .

Similar to Case 1 results, the increase on the number of individuals of all optimization techniques generates better fitness performance. When using a larger number of individuals, the final fitness values in each case improves for PSO and DE, but contrasting as results discussed in Section 5.1, PSO exhibits higher fitness values than DE assuming the function φ_2 with 16 and 32 individuals, shown in Figures 5.9b and 5.10b. The DE performance for function φ_2 indicates that the number of iterations is insufficient for performing optimization, which is evident in CDFs shown in Figure 5.7 when placing 2 new bases.

These results indicate that DE obtains better performance on optimization considering fitness function φ_1 while PSO expresses better advances with φ_2 .

8 Individuals

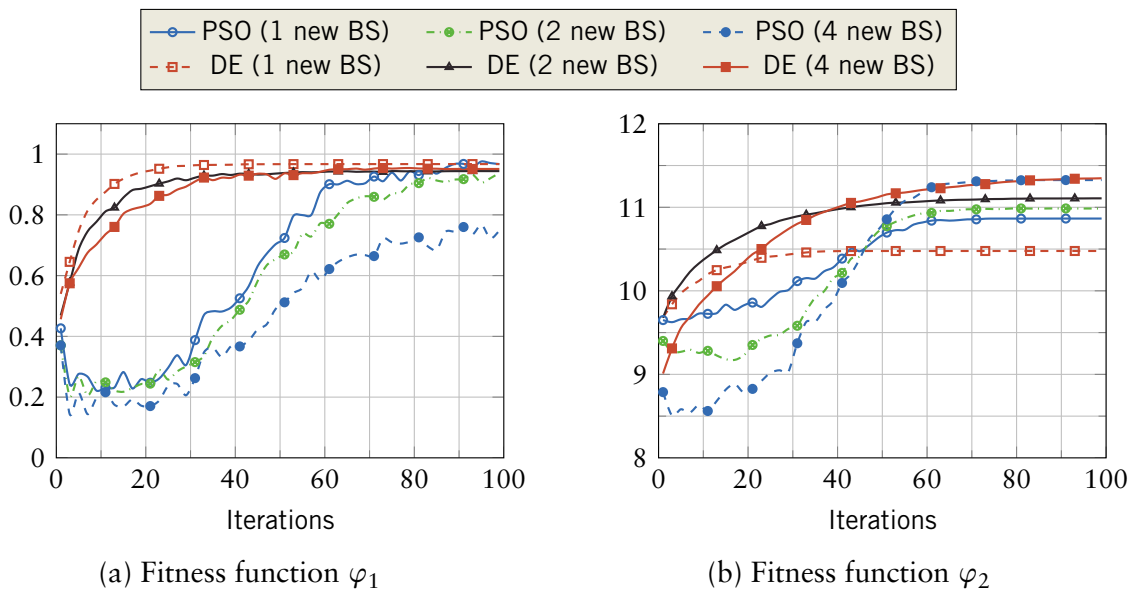


Figure 5.8: PSO and DE fitness performance for 8 individuals placing 1, 2 and 4 new BSs – Stochastic Geometry

5.2.2 Network Performance Metrics

In order to investigate optimization impact on BSP using metrics described in Section 4.7, Figure 5.11 show the influence of optimization process in these attributes when inserting 4 new bases.

16 Individuals

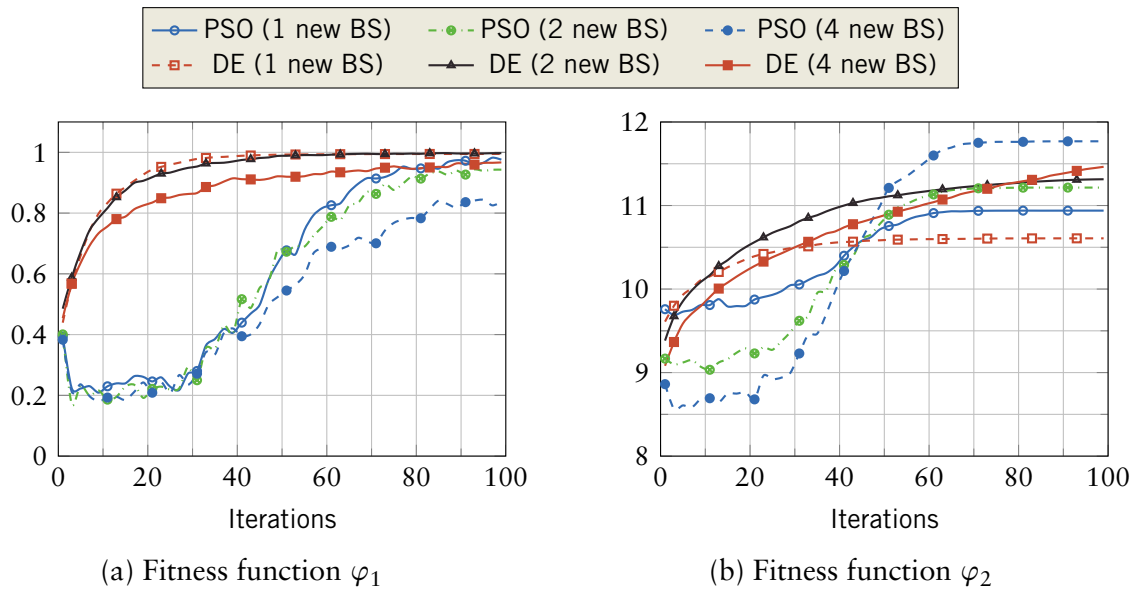


Figure 5.9: PSO and DE fitness performance for 16 individuals placing 1, 2 and 4 new BSs – Stochastic Geometry

32 Individuals

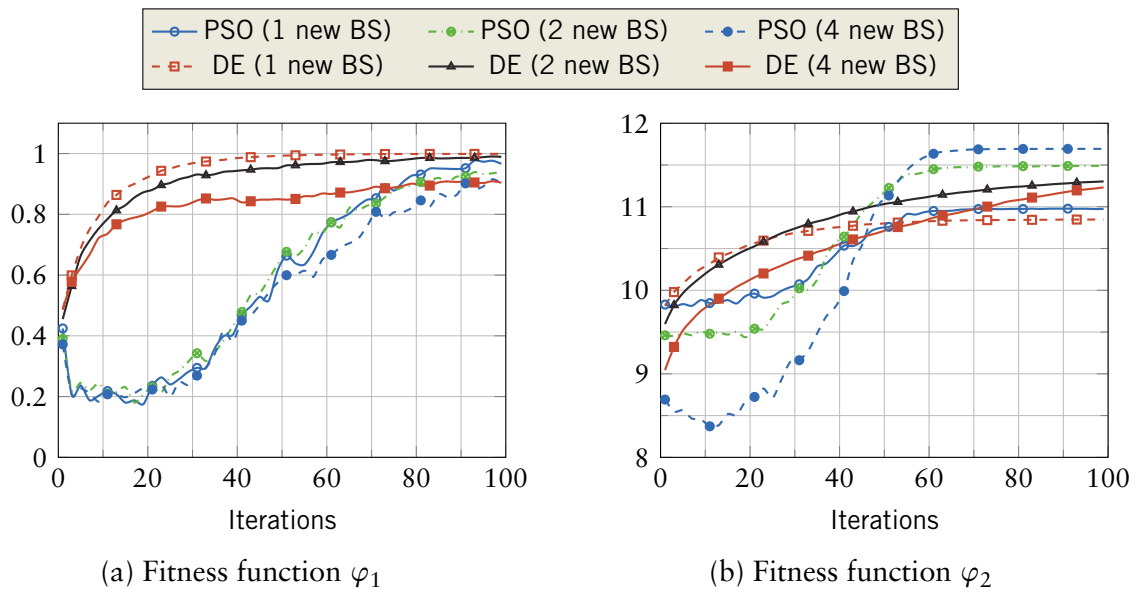


Figure 5.10: PSO and DE fitness performance for 32 individuals placing 1, 2 and 4 new BSs – Stochastic Geometry

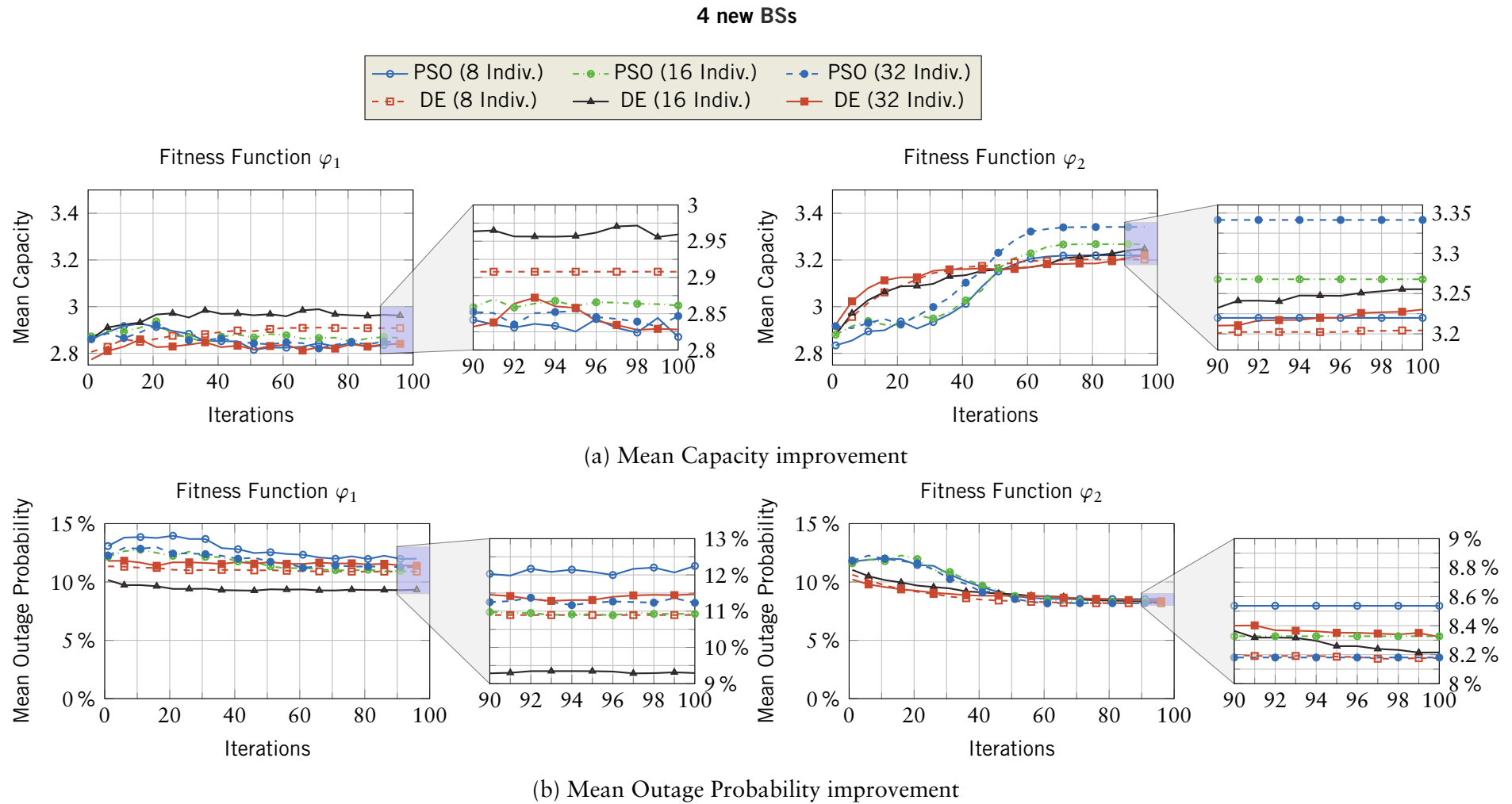


Figure 5.11: PSO and DE network performance for placing 4 new BSs with 8 and 16 individuals – Stochastic Geometry

The impact of placing different numbers of new bases for 32 individuals is shown in Figure 5.12, considering only the fitness function φ_2 for optimization. For both optimization methods, the higher the number of bases, the more the improvement on network metrics at the end of iterations, but DE does not improve as much as PSO on mean capacity, differently than when evaluating mean outage performance.

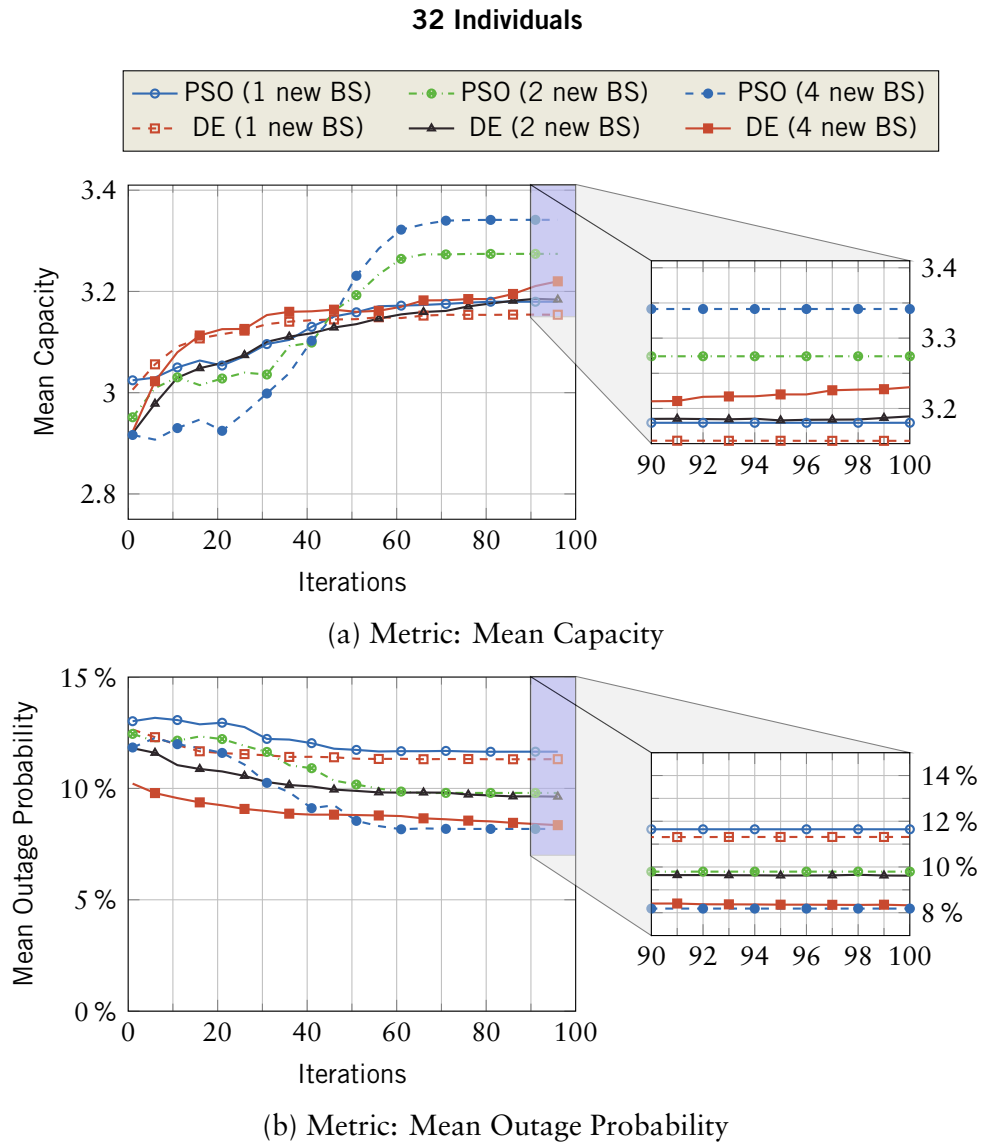


Figure 5.12: PSO and DE network performance for 32 individuals placing 1, 2 and 4 new BSs – Stochastic Geometry

The fitness function φ_1 does only a little contribution to the improvement on network metrics, thus, it is not effective to improve users' capacity, but it presents some enhancements on reducing mean outage of users.

On the other hand, the use of fitness φ_2 for optimization generates improvement on network metrics: the gain on users' mean capacity benefits more when using PSO than DE, when the number of iterations is fixed. In terms of mean outage probability, both

Table 5.6: Improvements on network metrics by optimization in SG layout – fitness function φ_2

Number of new BSs	Increase on number of BS	Mean Capacity		Mean Outage Probability	
		PSO	DE	PSO	DE
1	6.75%	3.86%	3.31%	-14.0%	-14.9%
2	13.1%	6.87%	6.65%	-23.9%	-26.3%
4	26.6%	11.0%	7.74%	-37.9%	-30.5%

methods result in similar improvement. The PSO also shows a higher increasing on mean capacity metric when using larger population size.

According to results obtained in previous subsection, DE does not present good performance on optimization using fitness function φ_1 , which does not result in improvements on network metrics. Thus, PSO is more efficient to optimize fitness φ_2 generating enhancements on network metrics capacity-based.

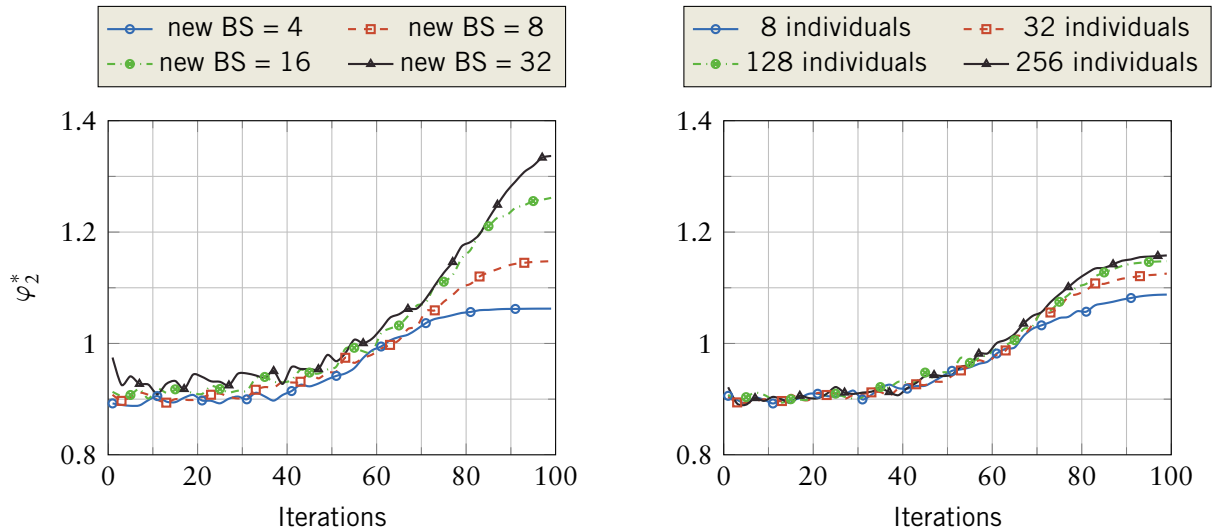
The improvement on infrastructure for placing 1, 2 and 4 new bases is 6.75%, 13.1% and 26.6%, respectively, which results in enhancements for mean capacity and mean outage probability shown in Table 5.6, considering 32 individuals for optimization process. These results confirm that PSO has better performance than DE in terms of mean capacity improvement, resulting on enhancements of 11% versus 7.74% of DE when placing 4 new bases. DE is more effective for reducing mean outage probability than PSO when placing 1 and 2 new bases, but as the number of new bases enlarges, PSO overtakes DE in performance.

5.3 Case 3 – Real Data Based

Using actual data from City 1 – Case 3 – described in Section 4.3, PSO performs optimization with variation on the number of new BSs for positioning and fixed number of 128 individuals considering the fitness function φ_2^* presented in Section 4.4.

The results shown in Figure 5.13a exhibits improvement of all objective functions for each number of new BS, which PSO is able to enhance φ_2^* : the more the amount of new BSs, the higher the fitness improvement. Considering only old BSs on the environment, the load distribution of traffic among bases, computed from (2.20) is fixed, thus, increasing the number of new BSs contributes to individuals to have more control of this parameter in the optimization process. On the other hand, increasing number of new BSs generates higher interference, thus, limit the gain on fitness function.

The use of more individuals increases performance with iterations on optimiza-



(a) Using 128 individuals for deploying 4, 8, 16 and 32 new BS

(b) Deploying 8 new BS with different number of individuals

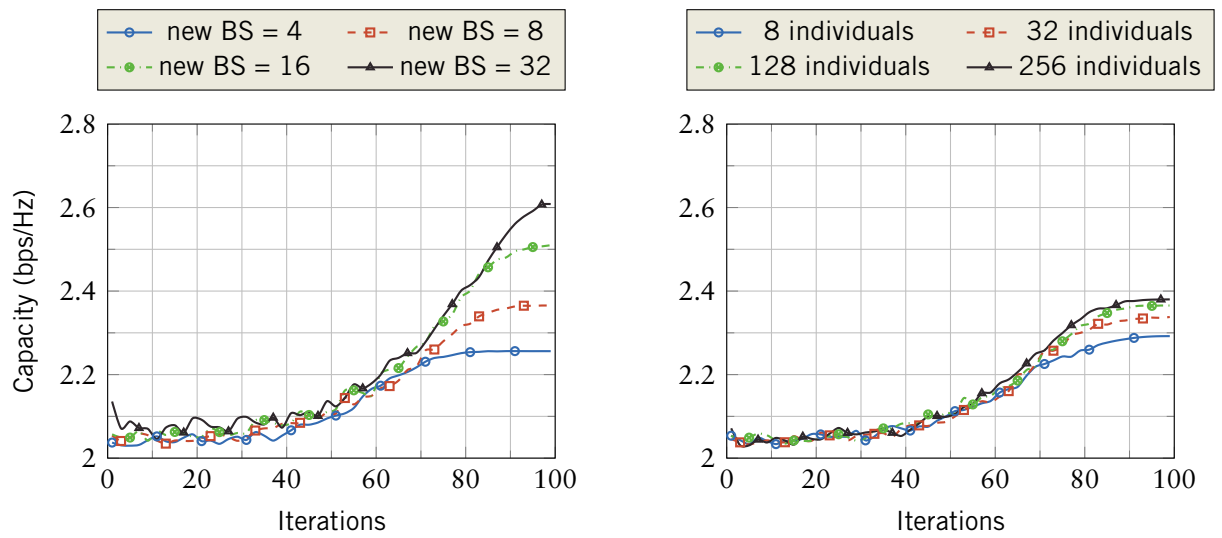
Figure 5.13: Fitness φ_2^* versus Iteration in Case 3

tion process. The enhancement on fitness function φ_2^* is shown in Figure 5.13b, which confirms that the use of a larger number of individuals for optimization affects fitness performance, but the use of 256 individuals enhances fitness by less than 0.4% as observed when using 128 individuals.

Considering network metrics, PSO enhanced system capacity by 17%, when increasing number of BSs by 8%, shown in Figure 5.14a. On the other hand, an increase of 32% of infrastructure resulted in an improvement of only 29.5% for capacity due to the higher interference in multiple BSs placement scenario.

When varying number of individuals, the enhances on capacity are shown in Figure 5.14b. Nevertheless, results for 256 individuals do not improve capacity more significantly than those observed for 128 individuals, resulting on enhancement by only 0.62%.

Finally, Figure 5.15 exhibit the distribution of the best points obtained in each trial for placing 8 new BSs, for 128 individuals, which corresponds to the most suitable regions for deployment of new BS. The overlapping of BS points, already placed infrastructure and peak traffic distribution of UE implies the PSO reaches regions with poor coverage and high traffic distribution, simultaneously.



(a) Using 128 individuals for deploying 4, 8, 16 and 32 new BS

(b) Deploying 8 new BS with different number of individuals

Figure 5.14: Capacity improvement *versus* Iteration in Case 3

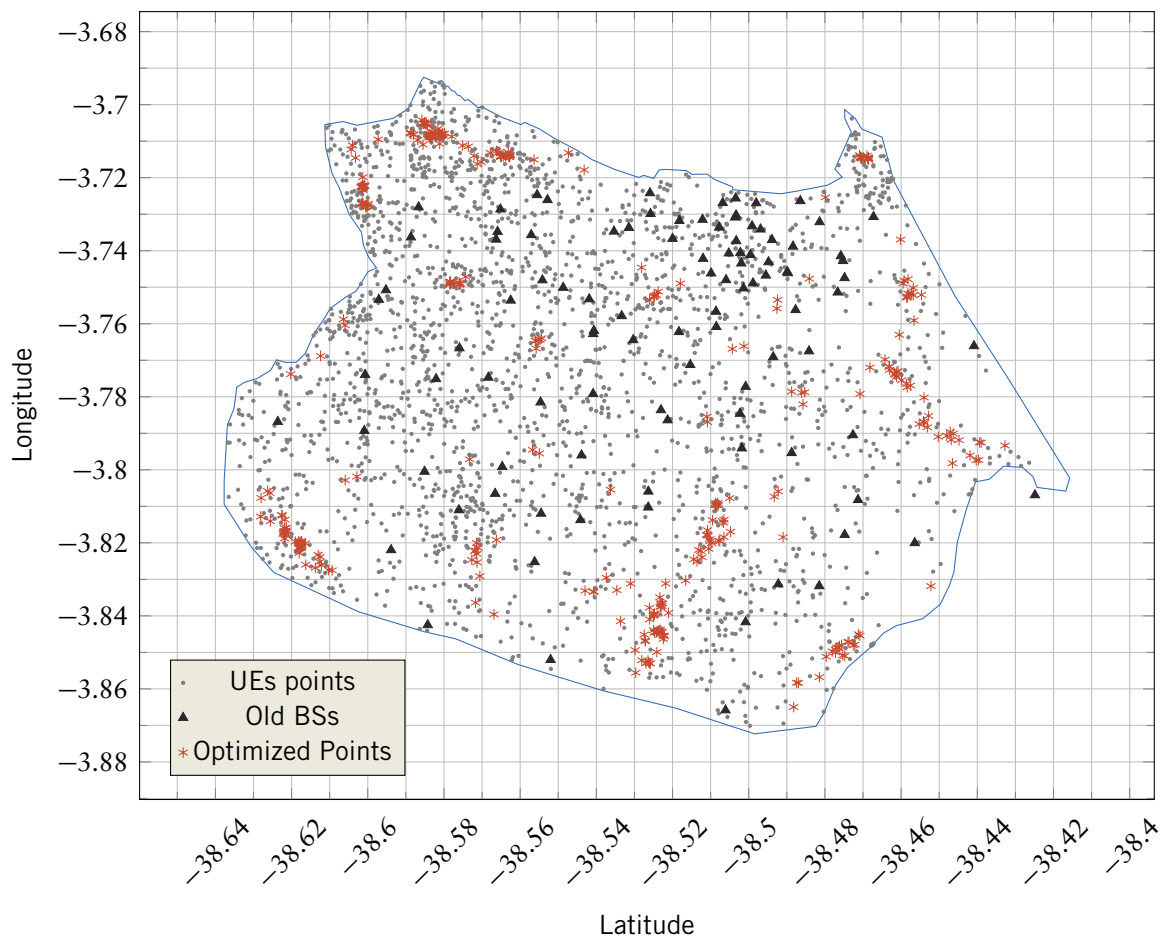


Figure 5.15: Optimized points for deploying 8 new BSs using 128 PSO individuals

6. CONCLUSION AND FUTURE WORK

THIS thesis has proposed a modelling of Base Station (BS) Placements (BSPs) optimization for Long Term Evolution (LTE)-Advanced (LTE-A) networks for infrastructure expansion considering, as major objectives, the maximization of traffic for users without overloading new bases and the increase of sensed capacities for users with load balancing using Particle Swarm Optimization (PSO) and Differential Evolution (DE) as heuristic methods. Chapter 2 presented some aspects of cellular networks used to compose two fitness metrics for optimization: as described in that chapter, these two metrics aim to improve performance of new placed nodes only or all network nodes respectively. Chapter 3 exhibited the PSO and DE as optimization methods, highlighting their aspects and some improvements for adjusting their performance. Chapter 4 showed modelling aspects for three scenarios: Grid, Stochastic Geometry (SG)-based and Actual data-based, from which users traffic also were modelled. The numerical results for BSP using PSO and DE were shown in Chapter 5.

Considering the simulation Case 1, the PSO exhibited better performance at the end of iterations for fitness functions φ_1 while DE presented better performance when working on fitness function φ_2 . The standard deviation of PSO's spatial points solutions was lower than those obtained by DE when using 32 individuals, although DE was able to result good performance after a fewer number of iterations. From simulation Case 2, the Stochastic Geometry-based scenarios, DE presented better performance when using few individuals for all fitness functions. As the number of individuals increases, PSO overtake DE in performance. It was verified that DE has better convergence time when using fitness function φ_1 in Case 2 simulation scenario. Considering the function φ_2 , PSO presented better fitness and network performance metrics as those observed with DE. Both methods were able to reduce mean outage probability for network when using the second fitness function. In Case 3, PSO was able to find solutions which optimized performance of fitness function φ_2^* when placing 8, 16 and 32 new bases in the environment. The improvement on mean capacity in some scenarios was higher than the increase on number of new bases.

The use of multi-objective requirements can be expanded for placement of nodes when energy efficiency is also a concern, such as the 5th Generation (5G) predictions. In this work, these heuristic methods were verified to be effective to find good solutions in environments where there are many parameters which affect fitness, heterogeneity of nodes and traffic distribution. The inclusion of energy efficiency metrics is a good start point when carry on using these methods as tool for assisting network planning.

REFERENCES

- [1] “Mobile apps overtake PC Internet usage in U.S.” [Online]. Available: <http://money.cnn.com/2014/02/28/technology/mobile/mobile-apps-internet/>
- [2] Ericsson, “Ericsson mobility report – on the pulse of the networked society.” [Online]. Available: <http://www.ericsson.com/res/docs/2014/ericsson-mobility-report-june-2014.pdf>
- [3] E. Hossain, M. Rasti, H. Tabassum, and A. Abdelnasser, “Evolution toward 5G multi-tier cellular wireless networks: An interference management perspective,” *IEEE Wireless Communications*, vol. 21, no. 3, pp. 118–127, June 2014. [Online]. Available: <http://dx.doi.org/10.1109/MWC.2014.6845056>
- [4] C. Soto, D. Covarrubias, and S. Villarreal, “Base station placement optimization algorithm for heterogeneous distributions of mobile users with multi-service requirements,” *IEEE Latin America Transactions*, vol. 10, no. 5, pp. 2032–2039, Sept 2012. [Online]. Available: <http://dx.doi.org/10.1109/TLA.2012.6362345>
- [5] S. Parkvall, A. Furuskar, and E. Dahlman, “Evolution of LTE toward IMT-advanced,” *IEEE Communications Magazine*, vol. 49, no. 2, pp. 84–91, February 2011. [Online]. Available: <http://dx.doi.org/10.1109/MCOM.2011.5706315>
- [6] 3GPP, “Requirements for Evolved UTRA (E-UTRA) and Evolved UTRAN (E-UTRAN),” 3rd Generation Partnership Project (3GPP), TR 25.913, Dec. 2009. [Online]. Available: <http://www.3gpp.org/ftp/Specs/html-info/25913.htm>
- [7] H. Holma and A. Toskala, *WCDMA for UMTS – HSPA evolution and LTE*, 4th ed. England, UK: John Wiley and Sons, 2007.
- [8] J. E. S. García, “Cost based optimization for strategic mobile radio access network planning using metaheuristics,” Ph.D. dissertation, Departamento de Teoría de la Señal y Comunicaciones, Escuela Politécnica Superior, Universidad de Alcalá, Madrid, ES., 2013.
- [9] L. Jia, W. Zhang, Z. Yang, C. Ma, and M. Chen, “Cell sites planning with minimized power consumption under cell load balancing constraint in LTE networks,” in *International Conference on Wireless Communications Signal Processing*, Oct 2013. [Online]. Available: <http://dx.doi.org/10.1109/WCSP.2013.6677145>
- [10] D. Amzallag, M. Livschitz, J. Naor, and D. Raz, “Cell planning of 4G cellular networks: Algorithmic techniques and results,” in *6th IEEE International Conference on 3G and Beyond*, Nov 2005.
- [11] B.-S. Park, J.-G. Yook, and H.-K. Park, “The determination of base station placement and transmit power in an inhomogeneous traffic distribution for radio network planning,” in *IEEE 56th Vehicular Technology Conference*, 2002. [Online]. Available: <http://dx.doi.org/10.1109/VETEFC.2002.1040579>
- [12] Y. Lin, W. Yu, and Y. Lohan, “Optimization of wireless access point placement in realistic urban heterogeneous networks,” in *IEEE Global Communications*

- Conference, Dec 2012. [Online]. Available: <http://dx.doi.org/10.1109/GLOCOM.2012.6503906>
- [13] J. Kennedy and R. C. Eberhart, "Particle swarm optimization," in *International Conference on Neural Networks*, vol. 4, Nov 1995. [Online]. Available: <http://dx.doi.org/10.1109/ICNN.1995.488968>
- [14] Z. Yangyang, J. Chunlin, Y. Ping, L. Manlin, W. Chaojin, and W. Guangxing, "Particle swarm optimization for base station placement in mobile communication," in *IEEE International Conference on Networking and Sensing and Control*, March 2004. [Online]. Available: <http://dx.doi.org/10.1109/ICNSC.2004.1297476>
- [15] D. Tsilimantos, D. Kaklamani, and G. Tsoulos, "Particle swarm optimization for UMTS WCDMA network planning," in *3rd International Symposium on Wireless Pervasive Computing*, May 2008. [Online]. Available: <http://dx.doi.org/10.1109/ISWPC.2008.4556215>
- [16] J. C. M. Feitosa, T. F. Maciel, E. M. G. Stancanelli, W. C. Freitas Jr., and F. R. P. Cavalcanti, "Particle swarm optimization for antenna port placement in coordinated multi-point systems," in *XXVII Simposio Brasileiro de Telecomunicacoes*, Sept 2009.
- [17] N. Aziz, A. Mohemmed, and B. Sagar, "Particle swarm optimization and voronoi diagram for wireless sensor networks coverage optimization," in *International Conference on Intelligent and Advanced Systems*, Nov 2007. [Online]. Available: <http://dx.doi.org/10.1109/ICIAS.2007.4658528>
- [18] K. Price, R. Storn, and J. A. Lampinen, *Differential Evolution — A Practical Approach to Global Optimization*. Berlin Heidelberg, New York: Springer, 2005.
- [19] S. Das, A. Abraham, and A. Konar, *Particle Swarm Optimization and Differential Evolution Algorithms: Technical Analysis, Applications and Hybridization Perspectives*. Berlin Heidelberg, New York: Springer, 2008.
- [20] S. Hojjatoleslami, V. Aghazarian, and A. Aliabadi, "DE based node placement optimization for wireless sensor networks," in *3rd International Workshop on Intelligent Systems and Applications*, May 2011. [Online]. Available: <http://dx.doi.org/10.1109/ISA.2011.5873254>
- [21] S. Haykin and M. Moher, *Modern Wireless communications*. Pearson Prentice Hall, 2005.
- [22] A. Goldsmith, *Wireless Communications*. Cambridge University Press, 2005.
- [23] T. S. Rappaport, *Wireless Communications: Principles and Practice*. New Jersey: Prentice Hall, 2002.
- [24] T. M. Cover and J. A. Thomas, *Elements of Information Theory*, 2nd ed. New Jersey: John Wiley and Sons, 2006.
- [25] P. Ameigeiras, Y. Wang, J. Navarro-Ortiz, P. Mogensen, and J. Lopez-Soler, "Traffic models impact on OFDMA scheduling design," *EURASIP Journal on Wireless Communications and Networking*, vol. 2012, no. 1, p. 61, 2012. [Online]. Available: <http://dx.doi.org/10.1186/1687-1499-2012-61>

- [26] D. P. Bovet and P. Crescenzi, *Introduction to the Theory of Complexity (Prentice Hall International Series in Computer Science)*. Prentice Hall PTR, 1994.
- [27] S. Boyd and L. Vandenberghe, *Convex Optimization*. Cambridge University Press, 2004.
- [28] R. K. Jain, D.-M. W. Chiu, and W. R. Hawe, “A quantitative measure of fairness and discrimination for resource allocation in shared computer systems,” Eastern Research Laboratory, Digital Equipment Corp., Tech. Rep., 1984. [Online]. Available: <http://www.cs.wustl.edu/~jain/papers/ftp/fairness.pdf>
- [29] J. Kennedy, *Encyclopedia of Machine Learning*. Springer Science+Business Media, 2011. [Online]. Available: <http://dx.doi.org/10.1007/978-0-387-30164-8>
- [30] O. Kramer, *A Brief Introduction to Continuous Evolutionary Optimization*, ser. SpringerBriefs in Applied Sciences and Technology: SpringerBriefs in Computational Intelligence. Springer International Publishing, 2014.
- [31] R. Poli, J. Kennedy, and T. Blackwell, “Particle swarm optimization,” *Swarm Intelligence*, vol. 1, no. 1, pp. 33–57, 2007. [Online]. Available: <http://dx.doi.org/10.1007/s11721-007-0002-0>
- [32] Y. Shi and R. C. Eberhart, “A modified particle swarm optimizer,” in *IEEE World Congress on Computational Intelligence*, May 1998. [Online]. Available: <http://dx.doi.org/10.1109/ICEC.1998.699146>
- [33] A. Ratnaweera, S. K. Halgamuge, and H. C. Watson, “Self-organizing hierarchical particle swarm optimizer with time-varying acceleration coefficients,” *IEEE Transactions on Evolutionary Computation*, vol. 8, no. 3, pp. 240–255, June 2004. [Online]. Available: <http://dx.doi.org/10.1109/TEVC.2004.826071>
- [34] R. Storn and K. Price, “Differential evolution – a simple and efficient heuristic for global optimization over continuous spaces,” *Journal of Global Optimization*, vol. 11, no. 4, pp. 341–359, 1997. [Online]. Available: <http://dx.doi.org/10.1023/A:1008202821328>
- [35] M. M. Ali and A. Törn, “Population set-based global optimization algorithms: Some modifications and numerical studies,” *Computers and Operations Research*, vol. 31, no. 10, pp. 1703–1725, Sep. 2004. [Online]. Available: [http://dx.doi.org/10.1016/S0305-0548\(03\)00116-3](http://dx.doi.org/10.1016/S0305-0548(03)00116-3)
- [36] 3GPP, “Evolved Universal Terrestrial Radio Access (E-UTRA); Further advancements for E-UTRA physical layer aspects,” 3rd Generation Partnership Project (3GPP), TR 36.814, Mar. 2010. [Online]. Available: <http://www.3gpp.org/ftp/Specs/html-info/36814.htm>
- [37] M. Haenggi, J. G. Andrews, F. Baccelli, O. Dousse, and M. Franceschetti, “Stochastic geometry and random graphs for the analysis and design of wireless networks,” *IEEE Journal on Selected Areas in Communications*, vol. 27, no. 7, pp. 1029–1046, Sep. 2009. [Online]. Available: <http://dx.doi.org/10.1109/JSAC.2009.090902>
- [38] H. ElSawy, E. Hossain, and M. Haenggi, “Stochastic geometry for modeling, analysis, and design of multi-tier and cognitive cellular wireless networks: A survey,”

- IEEE Communications Surveys Tutorials*, vol. 15, no. 3, pp. 996–1019, Third 2013. [Online]. Available: <http://dx.doi.org/10.1109/SURV.2013.052213.00000>
- [39] A. Guo and M. Haenggi, “Spatial stochastic models and metrics for the structure of base stations in cellular networks,” *IEEE Transactions on Wireless Communications*, vol. 12, no. 11, pp. 5800–5812, November 2013. [Online]. Available: <http://dx.doi.org/10.1109/TWC.2013.100113.130220>
- [40] “Agência Nacional de Telecomunicações.” [Online]. Available: <http://sistemas.anatel.gov.br/stel/consultas/ListaEstacoesLocalidade/tela.asp?pNumServico=010>
- [41] J. E. Bell, S. E. Griffis, W. A. C. III, and J. A. Eberlan, “Location optimization of strategic alert sites for homeland defense,” *Omega*, vol. 39, no. 2, pp. 151–158, 2011. [Online]. Available: <http://dx.doi.org/10.1016/j.omega.2010.05.004>
- [42] K. Tutschku, “Demand-based radio network planning of cellular mobile communication systems,” in *17th Annual Joint Conference of the IEEE Computer and Communications Societies*, Mar 1998. [Online]. Available: <http://dx.doi.org/10.1109/INFCOM.1998.662915>
- [43] “Prefeitura de fortaleza.” [Online]. Available: <http://www.fortaleza.ce.gov.br/regionais>
- [44] N. Instruments, “Introduction to LTE device testing – from theory to transmitter and receiver measurements,” National Instruments, Tech. Rep., 2010. [Online]. Available: http://download.ni.com/evaluation/rf/Introduction_to_LTE_Device_Testing.pdf
- [45] S. E. Elayoubi, M. K. Karray, Y. Khan, and S. Jeux, “A novel hybrid simulation methodology for capacity estimation in mobile networks,” *Physical Communication*, vol. 9, pp. 281–287, 2013. [Online]. Available: <http://dx.doi.org/10.1016/j.phycom.2012.07.001>